



Linking In-Canopy Chemistry to Above-Canopy O₃, BVOCs, and NO_x Gas Fluxes in the Amazon Rainforest

Flossie Brown^{1,*}, Colette L. Heald^{1,*}, Allison Steiner², Ana Maria Yáñez-Serrano^{3,4,5}, Jürgen Kesselmeier⁶, Carolina de A. Monteiro⁷, Hartwig Harder⁷, Alessandro C. de Araújo⁸, Denisi H. Hall⁹,
5 Cléo Quaresma Dias-Júnior¹⁰

¹Institute for Atmospheric and Climate Science, ETH Zurich, 8092 Zurich, Switzerland.

²Department of Climate and Space Sciences and Engineering, University of Michigan, Michigan, 48109, United States

³Institute of Environmental Assessment and Water Research, IDAEA-CSIC, Barcelona 08034, Spain

⁴CREAF, E08193 Bellaterra (Cerdanyola del Vallès), Catalonia, Spain

10 ⁵CSIC, Global Ecology Unit, CREAM-CSIC-UAB, E08193 Bellaterra (Cerdanyola del Vallès), Catalonia, Spain

⁶Multiphase Chemistry Department, Max Planck Institute for Chemistry, 55128 Mainz, Germany

⁷Department of Atmospheric Chemistry, Max Planck Institute for Chemistry, 55128, Mainz, Germany.

⁸Empresa Brasileira de Pesquisa Agropecuária, Belém, Brazil

⁹National Institute for Amazonian Research, Manaus, AM, Brazil

15 ¹⁰Federal Institute of Education, Science and Technology of Pará, PA, Brazil

Correspondence to: Flossie Brown (flossie.brown@env.ethz.ch) and Colette L. Heald (colette.heald@env.ethz.ch)

Abstract.

20 The forest canopy is a distinct chemical and dynamical environment compared to the atmosphere above, characterised by natural emissions, deposition processes, and chemistry that vary with height. However, the role of in-canopy chemistry and its influence on above-canopy concentrations of ozone (O₃) and bi-directional exchange of natural compounds are necessarily simplified within large-scale models. Whilst canopy models have been applied to temperate forests, there are few studies in tropical forests. Here, we apply the FORCAsT canopy column model to an Amazonian site. Simulation of the 2015 El Niño
25 shows that biomass burning enhances O₃ flux into the canopy, increases oxidation chemistry and elevates O₃ deposition to vegetation. Sensitivity tests show sesquiterpenes enhance O₃ chemical loss from approximately 3% of the total in-canopy losses to 10%–15%, but only marginally reduce the total canopy O₃ flux. Sesquiterpene canopy escape efficiency varies by 45%–55% across simulations, controlled by O₃ oxidation and vertical turbulence. For other biogenic volatile organic
30 compounds (BVOCs), pool-dependent emissions demonstrate greatest variability in escape efficiency with environmental conditions (monoterpenes 84%–95%, isoprene 95%). Average soil NO_x escape efficiency (40%–50%) is higher than many existing models suggest and exhibits a strong diurnal cycle that drives O₃ production, especially in the early morning, which may be important to consider in global atmospheric chemistry models. Overall, we highlight reactive BVOCs by inclusion of sesquiterpene emissions and reactivity as major sources of uncertainty in in-canopy chemistry and emphasise the critical role of turbulence in linking canopy processes to above-canopy atmospheric composition.



35 1. Introduction

The Amazon rainforest stretches across 7 million km² to form a vast ‘green ocean’ of trees; a continuous canopy of leaves in all directions. This surface plays a pivotal role in tropospheric chemistry, functioning as a dynamic interface that emits biogenic compounds and exchanges trace gases with the atmosphere above (e.g., Covey et al., 2021; Schmitt et al., 2023). Its most significant contributions include biogenic volatile organic compounds (BVOCs) and soil-emitted nitric oxide (NO), both of which influence atmospheric composition and chemistry. These compounds participate in photochemical reactions that lead to the formation of ozone (O₃), a short-lived climate forcer that adversely affects human health and vegetation. At the same time, O₃ is a key component in maintaining the atmospheric oxidation capacity, thereby regulating the lifetimes of numerous trace gases like BVOCs and methane (CH₄). These processes contribute to the formation of secondary organic aerosols (SOA), which influence the Earth’s radiative balance and climate system. Furthermore, the forest serves as a surface for the deposition of atmospheric constituents, transferring trace gases from the atmosphere to the ecosystem.

This pristine tropical forest is rapidly changing (Aragão et al., 2018). Human activities and associated climate change are transforming the once-uninterrupted landscape into one fragmented by fire and deforestation (Marengo et al., 2018; dos Reis et al., 2021). From these regions, urban and biomass burning pollution can be advected long distances, influencing the chemical environment far from the emissions source (Brown et al., 2022). In particular, when NO_x from biomass burning interacts with the rainforest’s naturally high BVOC emissions, it enhances the formation of O₃ (Pacífico et al., 2015; Pope et al., 2020). Elevated O₃, once transported into the canopy, can enter plant leaves, inhibiting growth and reducing carbon sequestration, threatening the rainforest’s productivity (Cheesman et al., 2024; Vieira et al., 2023). Understanding O₃ concentrations over forested landscapes requires knowledge on how the canopy controls release and uptake of BVOCs, their interaction with NO_x and the role of the canopy in removing O₃.

Whilst global models often represent atmosphere-biosphere chemical exchange as a deposition or emission at a single surface layer, below the closed canopy structure exists a chemically vibrant space, with both chemical and depositional transformations occurring before canopy emissions are released to the atmosphere. Beginning in the trunk space, NO emissions from the soil can saturate the lower canopy, reacting with low concentrations of O₃ transported from above (Visser et al., 2022). In the near-perpetual darkness of the closed canopy, this acts as a chemical loss of O₃ and converts NO to NO₂. As NO is transported vertically, it encounters increasing concentrations of O₃, VOCs, and their oxidation products, further converting NO to NO₂. Exchange fluxes of NO_x and O₃ with soils and trees were intensively studied in the Amazonian rain forest within the LBA project (Gut et al., 2002) confirming that the plant canopy reduces the escape of NO_x by consumption of NO₂ under the strong influence of stomatal control (Breuninger et al., 2013; Chaparro-Suarez et al., 2011; Gut et al., 2002). Since O₃ and NO₂ are, among several gases, subject to deposition in the canopy and at the soil surface, the canopy acts to reduce the amount of NO_x from the soil that escapes the canopy at the same time as removing O₃ (Ganzeveld et al., 2002).

Canopy emission rates in global models are often modified by a species-specific canopy escape efficiency to represent removal within the canopy before release. For soil NO_x, Yienger and Levy (1995) derive a function based only on leaf area index (LAI)

and stomatal area index (SAI) that implicitly assumes an NO:NO₂ ratio and no temporal variation. However, they highlight that chemistry occurring below the canopy can affect this ratio, and it remains an uncertainty in the parameterisation and assumed magnitude of deposition.

Similarly, O₃ losses within the canopy through deposition and chemistry are often highly parameterised, with chemistry neglected altogether or implicitly included within deposition schemes. At different sites, chemical loss is estimated to contribute anywhere from a minor fraction to 20% of O₃ loss in the canopy (Rummel et al., 2007; Visser et al., 2021, 2022). In the Amazon, Rummel et al. (2007) cannot explain nighttime chemical losses with soil NO alone and assume a significant contribution from reaction with advected pollutants. Additional research suggests an important role of sesquiterpenes in removing O₃ within the canopy (Isaacman-VanWertz et al., 2024; Jardine et al., 2011; Stroud et al., 2005). These highly reactive BVOC emissions have been measured in the Amazon, with both leaf and soil sources (Bourtsoukidis et al., 2018; Jardine et al., 2011) but are not regularly included in chemistry transport models due to their high reactivity and limited understanding of their chemical products.

Studies have proposed that accurate representation of NO_x and O₃ chemistry within the canopy is only possible with explicit canopy resolution. Especially in the tropics, strong gradients in trace gas vertical profiles are formed from low turbulence, allowing stable separation from the boundary layer overnight and in the trunk space (Chamecki et al., 2020; Freire et al., 2017; Serra-Neto et al., 2021). Stratification and the formation of microclimates can further cause processes to deviate from parameterisations. Makar et al. (2017) suggest gradients in light and turbulence within the canopy can reduce above-canopy O₃ concentrations by 12%. Similarly, Visser et al., (2021) find single-layer schemes currently employed by land surface models misrepresent diurnal variability and stomatal:non-stomatal partitioning of O₃ sinks due to missing effects from turbulence.

To prioritise development for large scale models, an overview of the factors affecting canopy escape efficiencies and O₃ removal within the tropical forest is required. This includes understanding the role of the above-canopy atmosphere in affecting processes below the canopy, for example through propagation of vertical turbulence or in response to upwind transport of precursors, as well as explicit quantification of the importance of chemistry below the canopy. This study evaluates the role of the canopy in controlling atmospheric composition within and above the Amazon forest using a resolved canopy column model. We compare a year with typical meteorology to one with more extreme conditions including higher fire activity to understand the role of transported pollution on O₃ removal, BVOC escape efficiency and soil NO_x escape efficiency compared to pristine conditions. This acts as a first step towards identifying the important processes for improved parameterisation of tropical forest behaviour in global models.

2. Methods

2.1. Observation data at the Amazon Tall Tower Observatory

We use the Amazon Tall Tower Observatory (ATTO) site (Andreae et al., 2015) as the location for study and evaluation of the column model. The site is a research facility within the Uatuma Sustainable Development Reserve, in the pristine Brazilian



100 Amazon, 150 km NE of Manaus city (2°S, 59°W). This location is predominantly upwind of the city, although SE–E wind can
bring pollution from biomass burning and agriculture, especially during the dry season (Pöhlker et al., 2019). The wet and dry
seasons occur during December – May and July – October, respectively, while November and June are considered transition
months. Daylight hours are 6:00 to 18:00 local time (UTC-4). The vegetation is old-growth forest, with an average canopy
height of 35 m and greatest leaf density around 25 m (Gomes Alves et al., 2023). Measurements were taken at the 80 m tower
105 (named the Instant tower, 2.1468° S, 59.0068° W), which has been in operation since 2012. Temperature, photosynthetically
active radiation (PAR), friction velocity (u_*), and wind speed and direction measurements are available continuously since
2012 in half-hourly intervals.

Column model simulations (see Section 2.2) of the ATTO site require forcing data of vertical wind standard deviation (σ_w),
 u_* , PAR, and wind direction which control mixing, temperature and light-related processes. Data from 1–13 November 2013
110 and 11–23 November 2015 are used in this study; these time periods were selected for maximum meteorological and chemical
data availability. Vertical wind standard deviation is not continuously available at the site and was not recorded during 2013.
Above-canopy observations are available from an intense campaign in 11–23 November 2015 at 55 m and 81 m. In-canopy
observations of σ_w were also measured at 24 m in a shorter period from 11–18 November 2015 (Dias-Júnior et al., 2019).

To validate our simulations, we compare model output to observed O₃ concentration measurements taken at the Instant tower
115 during November 2013 and 2015. This profile setup measures at 8 heights using a TEI 49i O₃ analyser. The lower part of the
vertical profile (0.05, 0.5 and 4 m above the forest floor) was set up on a tripod adjacent to the Instant tower. The upper part
of the vertical profile (12, 24, 38, 53 and 79 m) was mounted on the tower. Tubes were guided to a valve system switching
every 2 minutes between the different heights during the first three cycles within each hour, and every 1 minute and 30 seconds
during the last cycle, resulting in four measurements at each height per hour. The O₃ limit of detection (LOD) is 0.5 ppbv in
120 60 seconds.

Isoprene, monoterpenes (unspeciated) and isoprene oxidation products (MACR, MVK, ISOPOOH) were measured during 5
short campaigns from 2012 to 2015 (Yáñez-Serrano et al., 2015). Measurements were performed with a PTR-MS (Ionicon
Analytic GmbH, Austria) operated under standard conditions using the same profile set up as above. As the closest time periods
to that of our simulation, we use data from the campaigns in October 2015 and November 2012 as an observational reference
125 to compare to November 2015 and 2013, respectively. Sesquiterpenes have not been measured at the site.

2.2. Model description

We employ the FORCAsT v2 model (Ashworth et al., 2015; Wei et al., 2021), a multi-layer column model with explicit canopy
representation originally developed for the University of Michigan Biological Station (UMBS) site. Our set-up includes 18
canopy layers of increasing height, 20 soil layers, and an additional 22 above-canopy layers extending to 5 km. The model
130 timestep is 1 min with output archived every 30 mins. The model is forced by observations at 30 min intervals of wind direction,
 σ_w , u_* and PAR recorded above the canopy (Figs. S1, S2). For simulations of 2013, we duplicate σ_w from 2015 due to missing
observations, assuming that the average turbulence was similar between years. All other variables including temperature, wind



speed, chemistry, water and energy fluxes are computed by the model after specifying initial conditions. The minimal number of forcing variables is a feature of this canopy model, since many other canopy chemistry models are nudged by above-canopy observations. The model is described in detail by Ashworth et al. (2017), Wei et al. (2021) and Bryan et al. (2012); we provide a brief overview in what follows.

FORCAST v2 incorporates 576 chemical reactions involving 411 species, along with representation of emissions, deposition and basic advection. As in Wei et al. (2021), our simulations use the Caltech Atmospheric Chemistry Mechanism 3 (CACM3) with the Reduced Caltech Isoprene Mechanism (RCIM; Wennberg et al., 2018) to describe isoprene oxidation under low-NO_x conditions. Simple sesquiterpene chemistry is represented using β-caryophyllene oxidation by O₃, OH and NO₃ as a proxy for all sesquiterpenes (Table S1), with reactivity dominated by O₃. These reactions form a number of oxidation products including various peroxy radicals, HCHO, lumped organic acids, ketones and aldehydes, which continue to react with oxidants, NO, HO₂ and, in some cases, undergo UV photolysis (Wei et al., 2021). However, the reactivity and product formation from sesquiterpenes is highly uncertain due to lack of measurements.

Emissions of BVOCs follow the temperature- and light-dependent scheme of Guenther et al. (1995, 2012) with parameters adapted for the tropics. Soil NO emissions are temperature-dependent (Forkel et al., 2006).

Deposition to the canopy is simulated using a Jarvis-style model of stomatal conductance (Jarvis et al., 1999), with parameters defining the stomatal response to light, temperature, leaf water potential and humidity. Light penetration through the canopy is calculated for each layer and each leaf angle class, with sun and shade leaves represented (Norman, 1979). Deposition to the leaf surfaces and soil is calculated at each layer and is species dependent (Gao et al., 1993; Meyers and Baldocchi, 1988; Wesely and Hicks, 2000).

Advection of trace gases is represented using a simplified parameterisation in which the concentration of the advected species is increased at selected above-canopy model levels, scaled by wind speed and filtered by origin wind direction (Bryan et al., 2012).

Above the canopy, MOST theory is used to describe momentum, heat and mass transfer. Below the canopy, the decline in mixing closer to the ground (a result of surface friction and interception by the canopy) is calculated using K-theory (Raupach, 1989). This is a first-order closure theory that assumes that turbulent flow leads to transfer down a concentration gradient.

An eddy diffusivity coefficient (K) dictates the efficiency of turbulent mixing based on atmospheric stability (see SI Text S3). A canopy height (h) value of K is calculated using observations of σ_w (Sect. 2.1.), from which the in-canopy values are derived at each model level as σ_{w(z)} decreases with height z. Raupach et al. (1989) suggests scaling by an R factor to account for near-field effects, which describes changes to conditions close to an emissions source or boundary, especially from a non-uniform source:

$$R = \frac{1 - e^{-\frac{\tau}{Tl}} \times (\tau - Tl)^{3/2}}{(\tau - Tl \times e^{-\frac{\tau}{Tl}})^{3/2}} \quad \text{Eq. 1}$$

This equation describes the reduction of K explicitly. Tl is a scaling factor with units of length however τ is undefined and must be estimated. See SI Text S3 for further details.



2.3. Model set-up and initial conditions

We modify the vertical mixing profile within the canopy to create a faster reduction in mixing with height, reflecting a greater separation between the canopy and above-canopy in the tropical forest. To achieve this, we adapt the variation in σ_w with height within the canopy from a linear to a sine-based function, as suggested by Raupach et al. (1989) (Eq. 2). With this adjustment, measured in-canopy $\sigma_{w(24)}$ is reproduced from $\sigma_{w(h)}$, giving confidence in our estimation (Fig. S3, Fig. S4a). This implies that the vertical mixing can be described using only above-canopy observations, and therefore a longer period can be simulated.

$$\sigma_{w(z)} = 0.5 \times \sigma_{w(h)} + 0.45 \times \sigma_{w(h)} \times \cos\left(\pi \times \left(1 - \frac{z}{h}\right)\right) \quad \text{Eq. 2}$$

Transport of upwind NO_x from the Arc of Deforestation is accounted for in the advection scheme by adding NO_2 to heights 73 m – 200 m when the wind direction comes from $90^\circ - 150^\circ$, the wind direction coincident with higher O_3 measurements. The additional NO_2 concentration is scaled by wind strength so that higher concentrations are added when wind speed is high. Initial conditions at ATTO, including, initial temperature and O_3 concentrations, are based on observations recorded at the site. We initiate the simulation at midnight UTC, 20:00 local time; at this time most trace gas concentrations are low and do not need to be initialised.

Site-specific parameters are set for the conditions at ATTO, such as Jarvis parameters for stomatal conductance and a prescribed Leaf Area Index (LAI; m^2 leaf area / m^2 ground area) at each layer. LAI ($=5.3 \text{ m}^2 \text{ m}^{-2}$) and its vertical distribution at each layer is taken from November 2015 measurements at ATTO by Gomes Alves et al. (2023) (Fig. S4b). In cases where there are no observations for the tropics, parameters are left in their default state. These parameters describe the canopy structure, such as leaf angle, light reflectance and transmission through the canopy, and a leaf clumping factor, all of which can affect vertical temperature profiles and light penetration (Fig. S4c). Simulated vertical profiles of temperature are most sensitive to the clumping factor.

We set the light-dependent emission factor of isoprene to $6 \text{ nmol m}^{-2} \text{ s}^{-1}$ to reproduce observed maximum half hourly emissions of 6–10 $\text{mg m}^{-2} \text{ s}^{-1}$ (Gomes Alves et al., 2023). Other BVOCs (monoterpenes and sesquiterpenes) do not have measured emission rates so emission factors must be estimated based on concentrations. We represent α -pinene as a light-dependent (Kuhn et al., 2004a, b) and limonene as a temperature-dependent species based on observations at the ATTO site by Yáñez-Serrano et al. (2015), although the light and temperature dependence of tropical species emissions is currently not well characterised. Sesquiterpenes are emitted as 100% β -caryophyllene, given the currently limited understanding of these BVOCs. This is one of the most reactive sesquiterpenes and, although it is often measured to be among the most abundant (e.g., Costa et al., 2025; Gomes Alves et al., 2022; Jardine et al., 2011), it represents an upper limit on reactivity. The sesquiterpene emission factor is temperature-dependent and is set at $0.08 \text{ nmol m}^{-2} \text{ s}^{-1}$ at 25°C to match observed concentrations from Jardine et al. (2011) (Fig. S5). These measurements were taken at the nearby TT34 tower (2°S , 60°W) in the Amazon in 2010 (Jardine et al., 2011) as there are currently no tree- or leaf-level sesquiterpene measurements available at the ATTO site. Recent measurements at the ATTO site indicate that soils and cryptogams are very likely an additional source of sesquiterpenes



(Bourtsoukidis et al., 2018; Edtbauer et al., 2021). Soil NO emissions are corrected from previous model versions so that
 200 emissions are added to the lowest model layer.

We run 3-day sensitivity studies to identify the optimal vertical mixing parameter ($\tau/|T|$), sesquiterpene and monoterpene
 emission factors, and soil NO emission factors, as well as identify which uncertainties are most important to constrain (Table
 S2). The short-duration simulation avoids complications with model drift (e.g., build-up of species) as with previous uses of
 the model, which were limited to 2-days. The details of the sensitivity tests and comparison to literature are shown in the SI
 205 (Figs. S5–S9). As sesquiterpene emissions are highly uncertain and have the largest impact on O₃ concentrations, we test their
 contribution to chemistry further in the main simulations below.

Using the fitted parameters, we compare five simulations of the ATTO site in 1–13 November 2013 and 11–23 November
 2015 to explore effects of meteorology, sesquiterpenes and upwind transport of NO₂ in more detail (Table 1).

Simulation name	NO _x source	Sesquiterpene emission
2013	Soil NO	Yes
2013 No SQT	Soil NO	No
2015	Soil NO, transport of NO ₂	Yes
2015 No SQT	Soil NO, transport of NO ₂	No
2015 pristine	Soil NO	Yes

210 Table 1: Variables in 5 simulations investigating effects of NO_x sources and sesquiterpene emissions.

2.5. Canopy exchange calculations

To estimate a canopy exchange of NO_x and O₃ (E_x) from the canopy to the atmosphere, we use the formula defined in Rummel
 et al. (2007), which specifically accounts for temporary storage of trace gases within the canopy:

$$E_x = \int_0^h Chem_{net}(z)dz - \int_0^h Dep(z)dz + \int_0^h Emission(z)dz + \frac{d}{dx} \int_0^h [x](z)dz \quad \text{Eq. 3}$$

215 Where x is either O₃ or NO_x and each term describes the integrated sum of chemistry, deposition, emission and storage across
 the vertical canopy levels z from soil level to canopy height h .

In the case of NO_x in 2015, it is useful to further separate the canopy exchange into the contributions from transported NO₂
 and soil NO to calculate a canopy escape efficiency of soil NO_x. The contribution from upwind NO₂ transport into the canopy,
 $E_{NO_x,transp}$, is estimated as the canopy exchange from a simulation of 2015 with no soil NO. This contribution is removed from
 220 simulations that contain both soil NO and transported NO₂ to give the soil NO_x escape efficiency.

$$Escape_{NO_x} = E_{NO_x} - E_{NO_x,transp} \quad \text{Eq. 4}$$



3. Results

3. 1. Simulation Evaluation

November 2013 at the ATTO site was a typical month in terms of temperature and wind velocity (Schmitt et al., 2023).
225 November 2015 was atypical; El Niño conditions caused temperatures at ATTO to be 3 °C higher compared to 2013 and 1.5
°C higher across the Amazon compared to average (Jiménez-Muñoz et al., 2016). The 2015/16 El Niño drought reached
maximum intensity in October 2015, with forest fires in November continuing to burn as though it was still the dry season
(Ribeiro Neto et al., 2022; Silva Junior et al., 2019). During this period, the wind at ATTO predominantly originated from the
Arc of Deforestation in the East (Fig. S10a), the location of enhanced fire activity (Silva Junior et al., 2019).
230 Measurements of atmospheric composition at ATTO during November 2015 showed increased OH reactivity, monoterpene
emissions and oxidation product-to-isoprene ratios compared to previous years (Pfannerstill et al., 2018, 2021; Yáñez-Serrano
et al., 2015, 2018). Daily mean O₃ concentrations in November 2015 were elevated compared to previous years, reaching up
to 28 ppbv at 38 m, whereas 2013 concentrations varied between 4 and 16 ppbv at the canopy top, typical for the ATTO site
(Fig 1).
235 In our simulations, mixing below the canopy is enhanced in 2015 compared to 2013 during daytime (Fig. S4a). Vertical
turbulent exchange shows strongly decreased vertical mixing at night, with stable air throughout the canopy especially between
1:00–5:00 local time (5:00–9:00 UTC) in both years. By midday, the canopy is well-mixed down to the lowest 20%–30%,
which remains more separated from the air above (Fig. S11).
We evaluate temperature and wind in our simulations and find the model reproduces temperatures in 2013 and 2015 well
240 ($r^2=0.80$), albeit with a smaller diurnal range than observed and a stronger vertical gradient below the canopy (Fig. 1). Previous
applications of the FORCAST model also find the simulated diurnal variability is lower than observed (Wei et al., 2021). The
model captures the difference between years and the day-to-day variability (Figs. 1b, 1c). The horizontal wind profile within
the canopy is also reproduced, although the night-time wind speed is underestimated above the canopy (Fig. S12).
Measurements show windspeeds are maintained around 2–4 m s⁻¹ overnight at 70 m, whereas friction velocity, which controls
245 simulated wind speed, drops substantially, driving this underestimation. We find the meteorological performance of the model
at this site to be comparable to simulations of the temperate forest, even when extending the simulation time considerably from
previous 2-day studies (Wei et al., 2021).

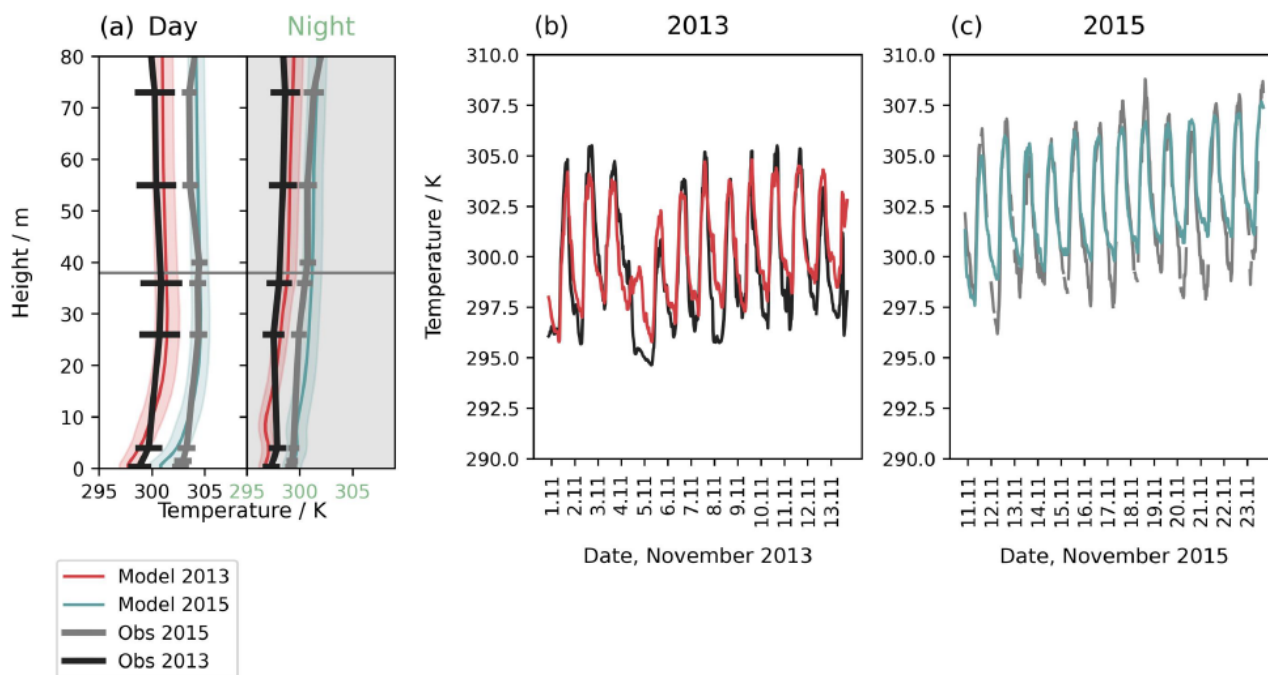
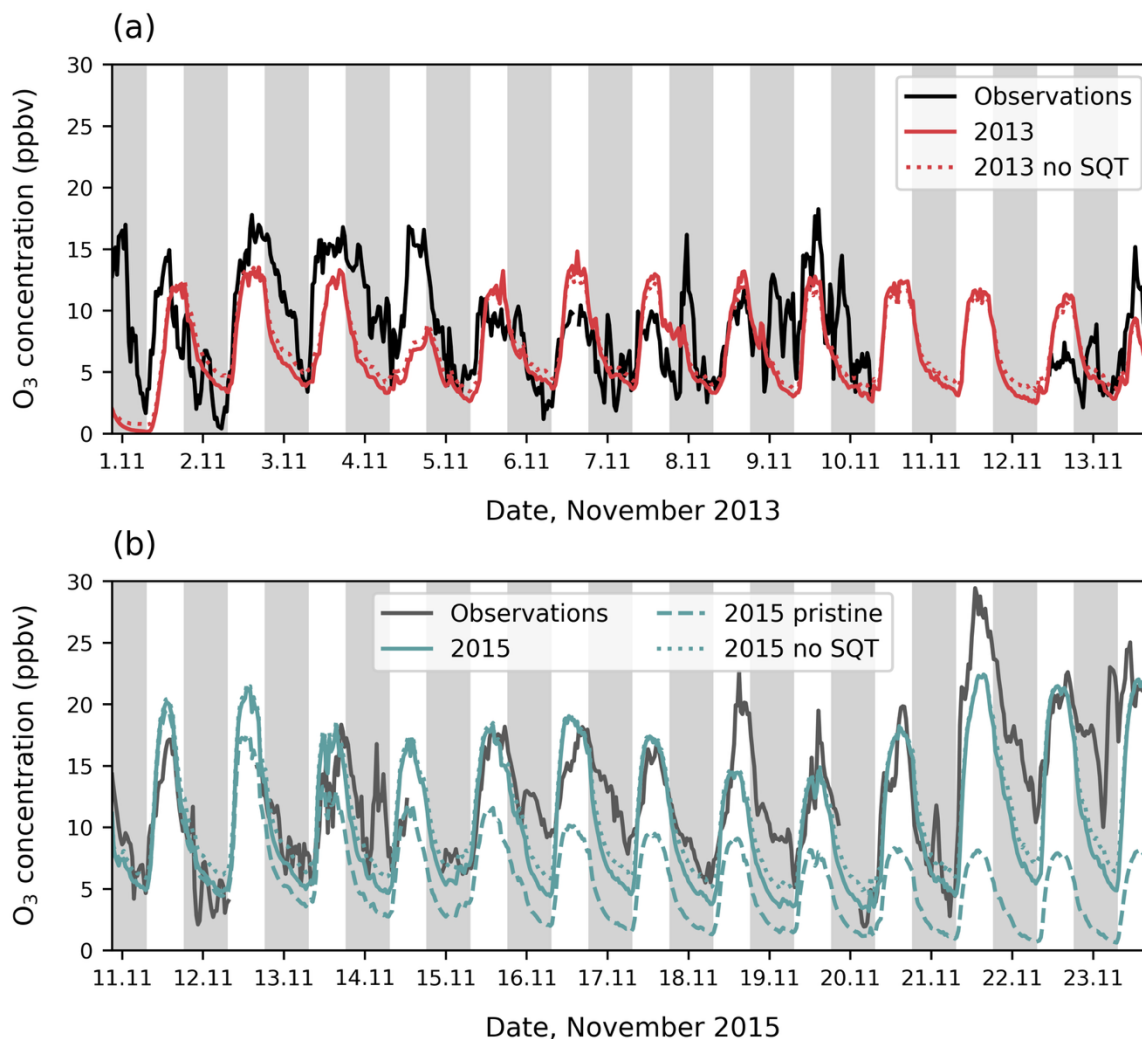


Figure 1: (a) Mean vertical profile of air temperature for day and night for simulations of 2013 (red solid line), 2015 (teal solid line) and observations in 2013 (black solid line) and 2015 (grey solid line). Horizontal lines and shading show the daily mean standard deviation. (b) and (c) show the time series evaluation at 36 m for (b) 2013 and (c) 2015.

Figure 2a shows the model can reproduce the general magnitude and diurnal cycle of O_3 concentrations in 2013. However, day-to-day variability is not well captured, especially the patterns in peak O_3 concentrations among different days. One of the vertical mixing components (σ_w) is not available for 2013, so day-to-day variability driven by mixing cannot be fully represented. In November 2015, the magnitude of measured O_3 concentrations can only be reproduced when upwind transport of NO_2 from fires is included (Fig. 2b). Without transported NO_2 , O_3 concentrations in 2015 are lower than 2013 concentrations despite higher temperatures, but when included, average O_3 concentrations over the 2015 simulation period are almost doubled. We find that inclusion of transported NO_2 captures the daily variability in peak O_3 concentrations on most days (Fig. 2b). This suggests that advected biomass burning air masses are the main driver of higher O_3 concentrations at the site in 2015 rather than the higher temperature.



265 Figure 2: Above canopy O₃ concentrations at 38 m from observations (solid black line) compared to simulations (coloured lines) for (a) November 2013 and (b) November 2015. Axis ticks are placed at midnight, and grey shading shows nighttime. In (a) simulations include O₃ concentrations with (red solid line) and without sesquiterpene emissions (red dotted line). In (b) simulations include O₃ concentrations when transport of NO₂ is included (teal solid line), without transported NO₂ (teal dashed line) and without sesquiterpene emissions (teal dotted line).

270

In both 2013 and 2015, the model performs worst overnight, often failing to capture nights in which O₃ is maintained at high concentrations, including in the lower canopy in 2015 (Fig. 3a). Sensitivity tests in which sesquiterpene emissions are switched off are 1–2 ppbv higher at night, providing a better match to observations on average but not necessarily capturing the day-to-day variability better (Figs. 1, 2a, 2b). This may suggest that sesquiterpene emissions or their reactivity with O₃ are overestimated in the model, although high nighttime O₃, such as on November 14th 2015, are more likely related to turbulent

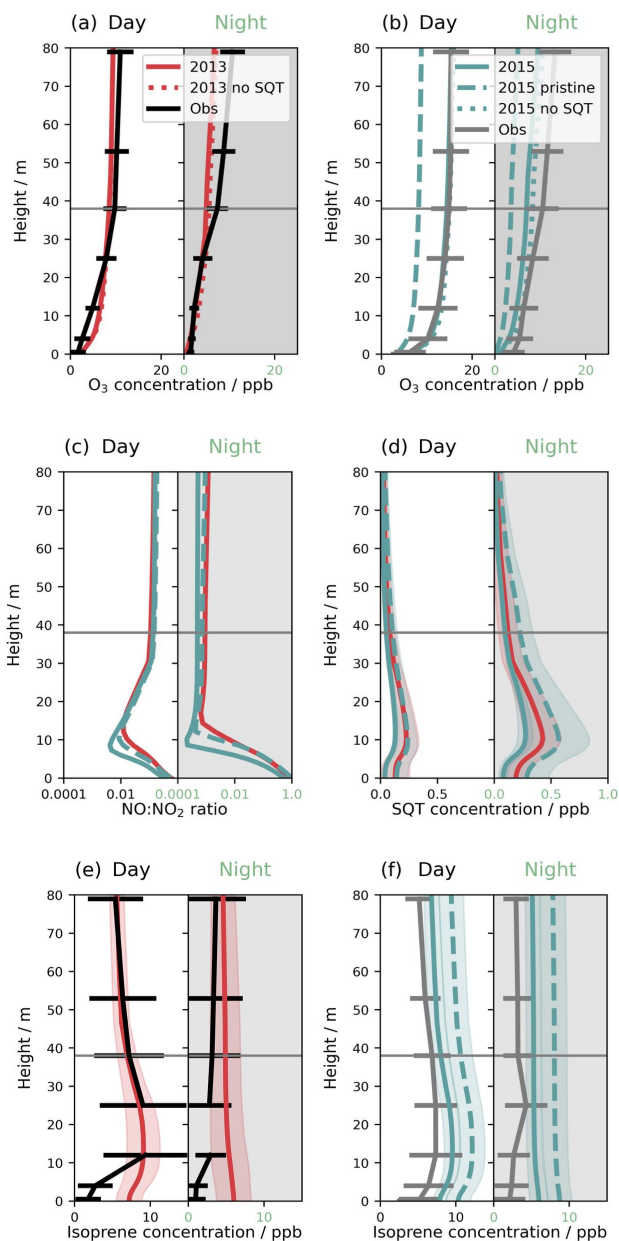
275



features (Fig. 2). The model captures the O₃ diurnal cycle more closely in the tropics compared to previously simulated temperate forests (Ashworth et al., 2015; Wei et al., 2021) due to the smaller influence from transported air masses at this site. Figures 2a and 2b confirm that, whilst the daytime O₃ profiles are a good match to observations, nighttime profiles are underestimated, especially above the canopy. In fact, the steeper gradient below the canopy in observations of 2013 suggests
280 some decoupling between the canopy and above that is not reproduced in the simulations. The lack of decoupling in the simulations likely contributes to the faster decline in above-canopy O₃ concentrations overnight compared to observations (Fig. 2). The shape of the daytime vertical profile in 2015 is better captured than in 2013; the observed 2013 vertical concentration gradient is steeper than 2015 but this is not replicated by the model.

Simulations of 2015 with transported NO₂, which produces additional O₃, consequently have a higher oxidative capacity. In
285 pristine conditions, daytime OH concentrations above the canopy are approximately 0.4x10⁶ cm⁻³, decreasing to 0.25x10⁶ cm⁻³ within the canopy (not shown). The addition of transported NO₂ increases OH by 2x above the canopy, with diminishing differences between simulations below the canopy.

Transported NO₂ is also associated with a change in the NO:NO₂ ratio (Fig. 3c) in the lower canopy. In pristine conditions, the NO:NO₂ ratio is 0.5 and 1 at the soil surface in the day and night, respectively, decreasing to 0.35 (day) and 0.5 (night)
290 when NO₂ transport is included in 2015. The elevated O₃ concentrations expedite the cycling of NO to NO₂, which removes NO in the dark lower canopy. By 10 m height within the canopy, NO concentrations are near zero in all simulations; NO is only re-formed closer to the canopy top where daytime photolysis is possible. Transported NO₂, of which very little reaches the soil level, does not strongly affect the NO:NO₂ ratio and the above canopy ratio does not depend strongly on the simulation.



295

300

Figure 3: Mean vertical profiles for day and night in simulations of 2013 (red solid line), 2015, including transported NO₂ (teal solid line) and 2015 without transported NO₂ (teal dashed line) for (a) O₃ in 2013, (b) O₃ in 2015, (c) NO:NO₂ ratio, (d) sesquiterpene concentrations, (e) isoprene concentration in 2013 and (f) isoprene concentration, in 2015. Simulations are compared to observations (a) of O₃ in November 2013 (black solid line), (b) of O₃ in and November 2015 (grey solid line), (e) of isoprene in November 2012 (black solid line) and (f) of isoprene in October 2015 (grey solid line). Error bars and shading show one standard deviation of daily means. The grey horizontal line indicates the canopy height.



High temperatures and PAR in 2015 increase BVOC emission compared to 2013; isoprene emissions increase by 50% and sesquiterpenes by 35% (Fig. S13). However, the concentration profiles (Figs. 2d–2f) are also related to background chemical composition. Simulations of 2015 in pristine conditions have higher BVOC concentrations compared to those with transported NO₂, as the lower oxidative capacity in pristine conditions leads to slower oxidation. With NO₂ transport included in 2015, isoprene concentrations are similar to 2013 concentrations, in both simulations and observations. The higher emissions in 2015 are balanced by increased oxidation. Concentrations of sesquiterpenes are lowest in 2015; the increased loss from the higher O₃ concentrations outweighs the increase in emissions (Fig. 3c). In all simulations, sesquiterpenes build up overnight within the canopy as vertical mixing declines and oxidation decreases, leading to higher concentrations at night compared to during the day in agreement with observations (Jardine et al., 2011).

Very low isoprene concentrations are recorded below the canopy (Fig. 3e, 2f) that are consistently overestimated by the model. Some studies find isoprene loss fluxes to tropical soils (e.g., Pugliese et al., 2023) that are not explored in this study.

3.2. O₃ losses in the canopy

Figure 4a shows the total canopy flux of O₃ divided into net chemical loss and deposition. The O₃ mostly originates from above the canopy, meaning the canopy is a net O₃ sink. The total flux in 2013 is -2.4 nmol m⁻² s⁻¹ compared to -3.9 nmol m⁻² s⁻¹ in 2015, whereas the total flux in 2013 and an idealised 2015 with no transported NO₂ are very similar. This implies the chemistry in the canopy is not strongly affected by the temperature changes between years, nor the deposition affected by other meteorological differences.

In all cases, deposition accounts for the majority of O₃ losses but the fraction of total loss that is due to chemistry is slightly higher in simulations without transported NO₂ at 15% compared to 11% when transport of NO₂ is included (Fig. 4a). Without sesquiterpenes the fraction of O₃ loss due to chemistry reduces to 3%–4%, however the decrease in chemical flux is partly compensated by an increase in deposition flux. This may suggest that sesquiterpenes can reduce deposition to vegetation and thus have the potential to reduce O₃ damage to vegetation. On the other hand, since the difference in the total flux is small, it indicates that the total O₃ in-canopy loss is somewhat resistant to uncertainties in sesquiterpene emissions and chemistry.

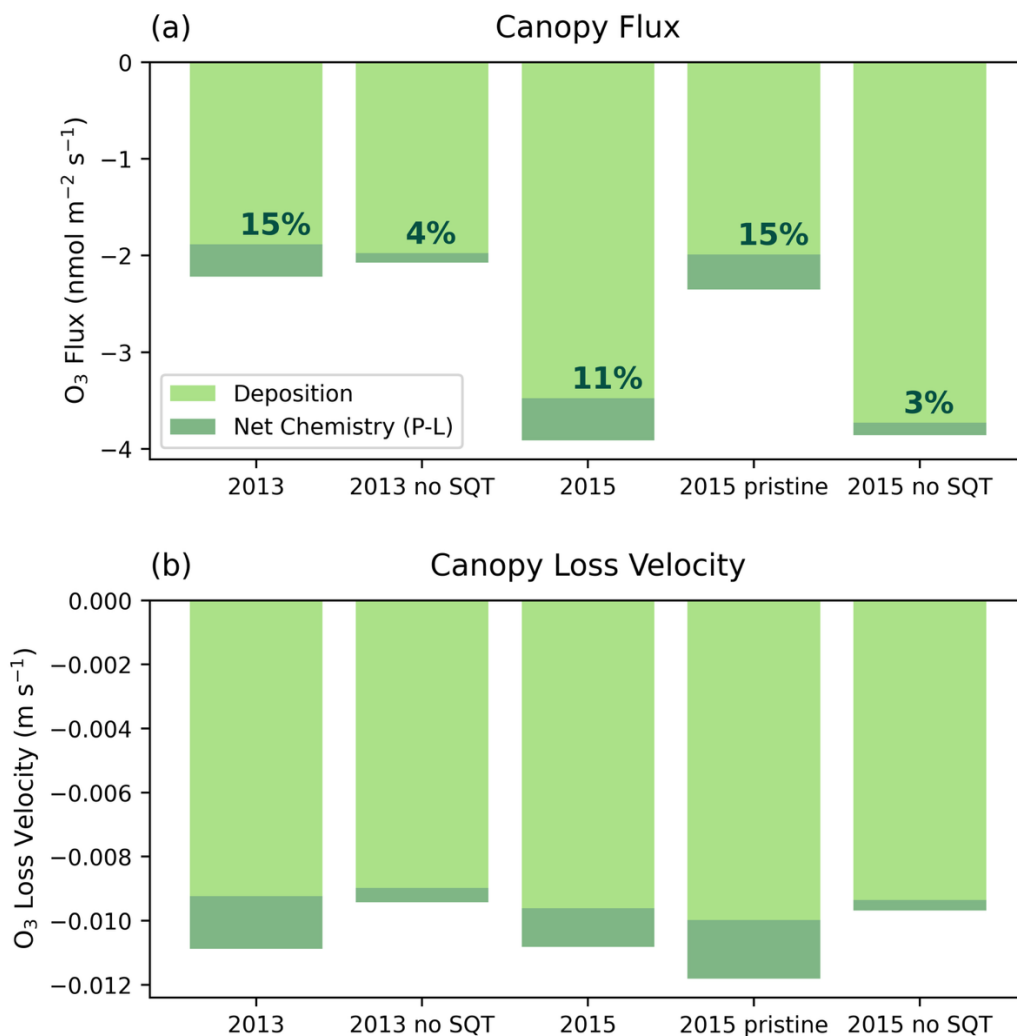


Figure 4: (a) The mean flux of O₃ in nmol m⁻² s⁻¹ and (b) the loss velocity in m s⁻¹ to the canopy divided into deposition (light green) and net chemistry (dark green). Text given in (a) indicates the percentage of loss that is chemical destruction.

330

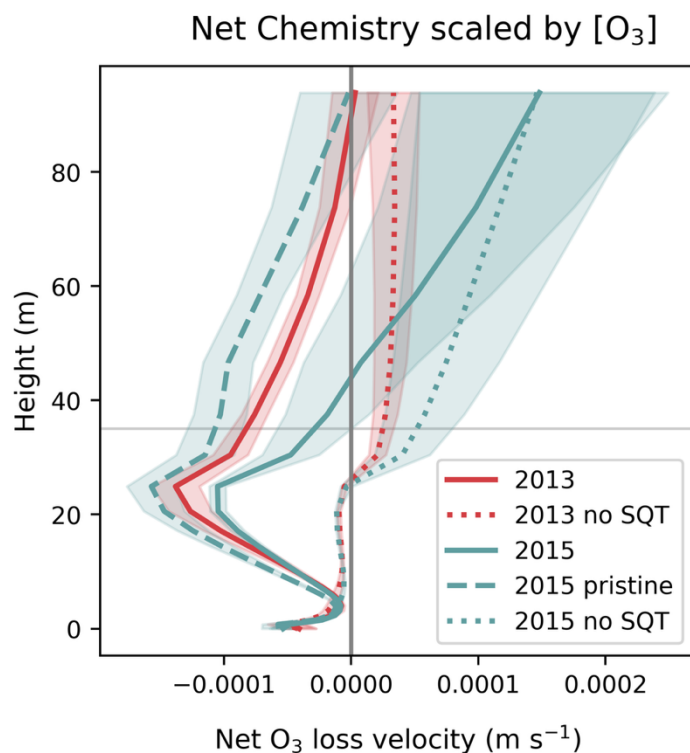
Figure 4b shows the equivalent losses scaled by O₃ concentration to obtain a canopy loss velocity. Variability in the loss velocity is much smaller than in the total O₃ flux, with a range of -0.009 to -0.012 m s⁻¹ among the simulations, implying that most of the difference in flux is related to differences in the O₃ concentrations. The major differences are (1) a small additional -0.0004 m s⁻¹ in deposition velocity between 2013 and pristine 2015, (2) an increase in chemical loss velocity in the absence of transported NO₂ in 2015, and (3) a decrease in chemical loss velocity without sesquiterpene chemistry.

335

Whilst the simulated O₃ fluxes are lower than measurements recorded in the Amazon by Rummel et al. (2007), the simulated deposition velocities are within the range of wet season observations but are higher than dry season averages of ~0.005 m s⁻¹ (Rummel et al., 2007). This may be due to reduced stomatal limitation as November is a transition month into the wet season.



Diurnal patterns of individual flux terms (chemistry, deposition and storage) show the same features identified by Rummel et al. (2007) such as an increase in storage in the morning as vertical transport brings O_3 into the canopy from above (Fig. S14). The vertical profiles of net chemistry in Fig. 5 elucidate the role of BVOCs and soil NO in driving O_3 losses within the canopy. In addition to removal by BVOCs in the canopy, soil NO is responsible for O_3 removal at the lowest model level, which compares to the reports from another Amazonian site (Gut et al., 2002). The chemical loss velocity profiles for simulations without sesquiterpene emissions show that loss by reaction with soil NO is of similar magnitude to O_3 removal by other BVOCs and the in-canopy profiles are very similar between years, which suggests sesquiterpenes are responsible for the differences in net chemistry. We find that consideration of both sesquiterpene emissions and O_3 concentrations are required to explain the canopy average loss velocity; there is a robust but non-linear relationship between canopy O_3 chemical loss and the ratio of sesquiterpene emissions to O_3 concentrations at 30 min resolution (Fig. S15). A decrease in chemical loss in 2015 in polluted conditions can be explained by an increase in O_3 concentrations, and faster losses in 2015 in pristine conditions can be explained by an increase in sesquiterpene emissions compared to 2013, on account of higher PAR and temperature. Differences between simulations are greatest at 20–25 m where the leaf area density (and associated BVOC emissions) is highest, whereas at the soil surface, chemical loss frequencies are similar.

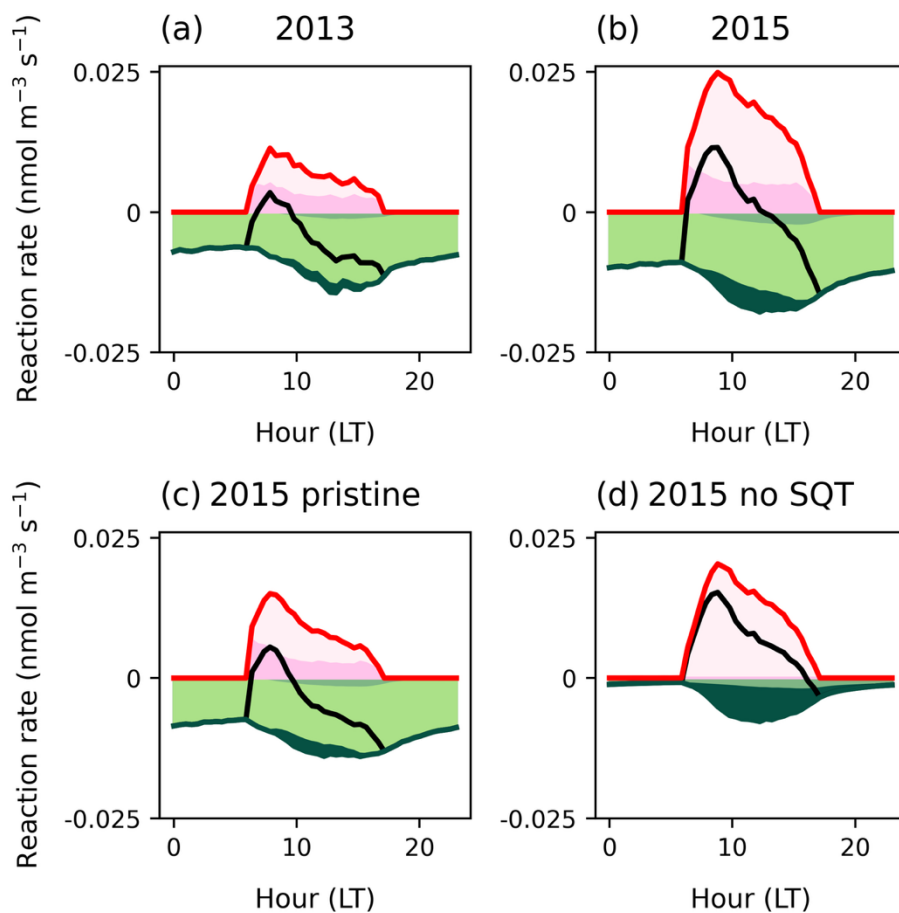
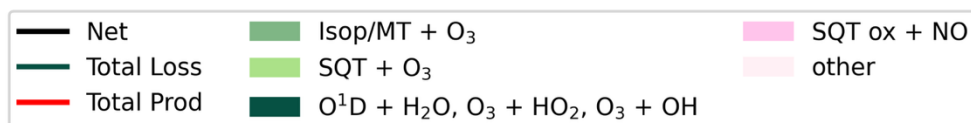


355 Figure 5: Vertical profiles of simulated net O_3 chemistry (production – loss) divided by O_3 concentration to give the loss velocity per molecule for simulations in 2013 (red lines) and 2015 (teal lines). Sensitivity tests show simulations without



sesquiterpenes (dotted lines) and 2015 without transport of NO₂ (teal dashed line). The horizontal line indicates the canopy top height.

- 360 Figure 6 shows the diurnal cycle of chemical production and loss occurring at 25 m, to demonstrate how chemistry varies over the day at the bulk canopy height (Fig. S4b). Considering the individual reactions involved in O₃ chemical loss (Fig. 6, green shading), sesquiterpene ozonolysis dominates at all times of day and is entirely responsible for nighttime chemistry at this height. Other BVOCs contribute to O₃ destruction during the afternoon and 2015 has a more substantial morning contribution from radical losses. Considering the whole canopy, over the diurnal cycle, chemistry is most important during the night, where
- 365 it can account for 40% the total O₃ losses (Fig. S14). During the day, the contribution diminishes to 5%, which is in response to an 8-fold increase in deposition rather than a significant change in chemistry.



370 Figure 6: Mean diurnal cycles at 25 m of chemical reactions for O₃ loss (green solid line), production (red solid line) and net chemistry (black solid line). Individual reactions are shaded showing sesquiterpene ozonolysis (light green shading), isoprene / monoterpenes + O₃ (medium green shading) and inorganic O₃ loss (dark green shading). For O₃ production reactions, β-carophyllene oxidation products is the largest uncertainty (pink shading).

375 The diurnal cycle reveals that even at 25 m, simulations switch to net O₃ production after sunrise and the breakdown of the nighttime boundary layer (approx. 6am) (Fig. 6, black solid line). O₃ production (Fig. 6, red solid line) is driven by a large number of oxidation products in the presence of NO; the three largest contributors are isoprene oxidation products, HO₂ and sesquiterpene oxidation products. As the largest uncertainty, the contribution from sesquiterpene oxidation products is shown in dark pink shading; it counteracts a substantial portion of daytime losses due to sesquiterpenes at this height. Production is smallest in 2013 and enhanced in the presence of transported NO_x (Fig. 6b) such that net production of O₃ continues until



380 13:00 on average compared to until 10:00 in pristine conditions (Fig. 6c). Without sesquiterpenes, net O₃ production occurs throughout daylight hours (Fig. 6d). The significant diurnal variability in O₃ production suggests that canopy escape efficiencies of precursors (especially NO_x and sesquiterpenes) should be investigated across the diurnal cycle.

Using the mean vertical profile, the transition to net O₃ production occurs at different heights among simulations (Fig. 5). Addition of transported NO₂ triggers net production at 40 m whereas in pristine conditions, profiles in 2013 and 2015 both show net loss of O₃ up to 100 m. Without sesquiterpene emissions, net O₃ production begins immediately above the main canopy density at 25 m, where light is not strongly attenuated and can initiate photolysis (Fig. S4c). Simulations with and without sesquiterpene emissions converge at around 100 m, indicating the point at which sesquiterpenes are fully oxidized. A significant portion of O₃ losses by sesquiterpenes occur above the canopy, implying that accurate quantification of sesquiterpene escape efficiencies is important for above canopy chemistry.

390

3.3. The role of BVOCs in canopy chemistry

The escape efficiency of sesquiterpenes ranges from 45%–55% between simulations. The highest escape efficiency of 55% occurs in 2015 pristine conditions. When transport of NO₂ is included, this decreases to 48% as a result of higher O₃ concentrations. Both simulations of 2015 have a higher escape efficiency than the 45% in 2013.

395 The MEGAN 2.0 BVOC emissions model includes an escape efficiency to account for BVOC losses within the canopy, based on chemical lifetime, u_* and canopy depth (Guenther et al., 2006). This parameterisation results in canopy escape efficiencies from 10% (in the presence of high O₃) to 60%. Our results, in relatively low O₃ conditions compared to global averages, fit realistically within this wide range. We find daily mean escape efficiency is best described using the eddy diffusivity coefficient K, rather than u_* , and O₃ concentration, which is inversely proportional to the chemical lifetime ($r^2=0.74$, $p<<0.05$; Fig. S16a).

400 Whilst a significant correlation still exists between escape efficiency and u_* ($r^2=0.69$, $p<<0.05$; Fig. S16b), the correlation is lower as K also includes information on vertical mixing through σ_w . In 2013, u_* is not an indicator of escape efficiency ($r^2=0.01$), whereas in 2015 the difference in performance is smaller. This indicates that the current equation in MEGAN 2.0 is functional assuming that u_* is correlated with vertical mixing, although may be improved by using K when possible.

Isoprene and α -pinene escape efficiencies are 95% both with and without transported NO₂, and in both 2013 and 2015. This is despite different emission magnitudes of isoprene of 4.7 and 7.3 mg m⁻² s⁻¹ due to varying meteorological conditions (Fig. S13). The isoprene escape efficiency of 95% with little variability is consistent with the parameterisation from MEGAN 2.0 (Guenther et al., 2006).

Conversely, limonene escape efficiency is slightly more sensitive to the environmental conditions, with escape efficiencies of 88% in pristine conditions in 2015, dropping to 84% with transported NO₂ and in 2013. These temperature-dependent pool emissions continue overnight when vertical mixing is slow, which allows more time for chemistry to act. This allows for greater differences in escape efficiencies due to chemical environments that are overcome during the day when vertical mixing is highly efficient and canopy residence times are short.

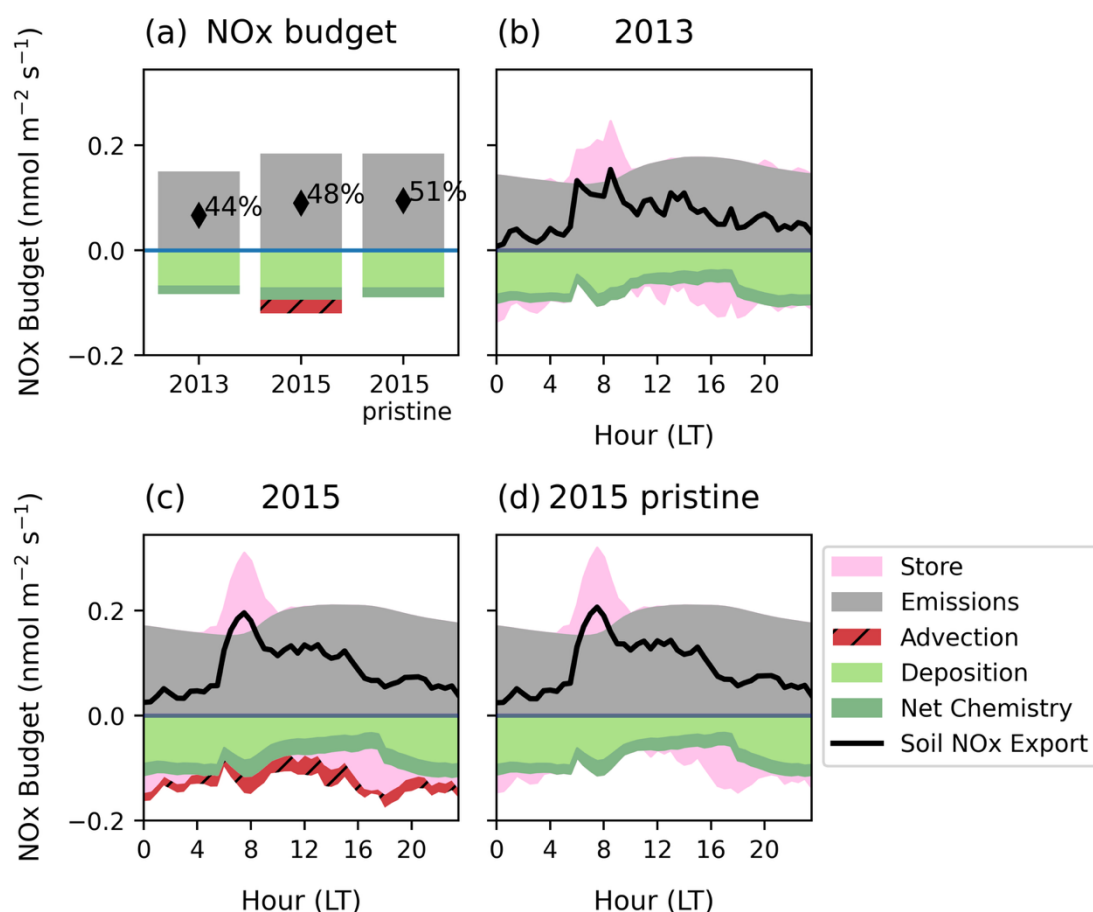
410



3.4. NO_x exchange with the canopy

3.4.1. Soil NO_x escape efficiency

415 Figure 7a shows the NO_x budget terms below the canopy and the overall escape efficiency of soil NO_x. The escape efficiency
 is different than the flux in that it excludes the contribution from upwind transported NO₂ into the canopy. We find the 2013
 escape efficiency of 44% is lower than 2015 simulations, given the consistent deposition of 0.7 nmol m⁻² s⁻¹ across simulations
 despite lower emissions in 2013. Comparing 2015 with and without transported NO₂ suggests the change in chemical
 environment due to upwind NO₂ transport has a relatively smaller effect on soil NO_x escape (48% vs 51%) and therefore
 420 escape efficiency is more dependent on meteorological changes.

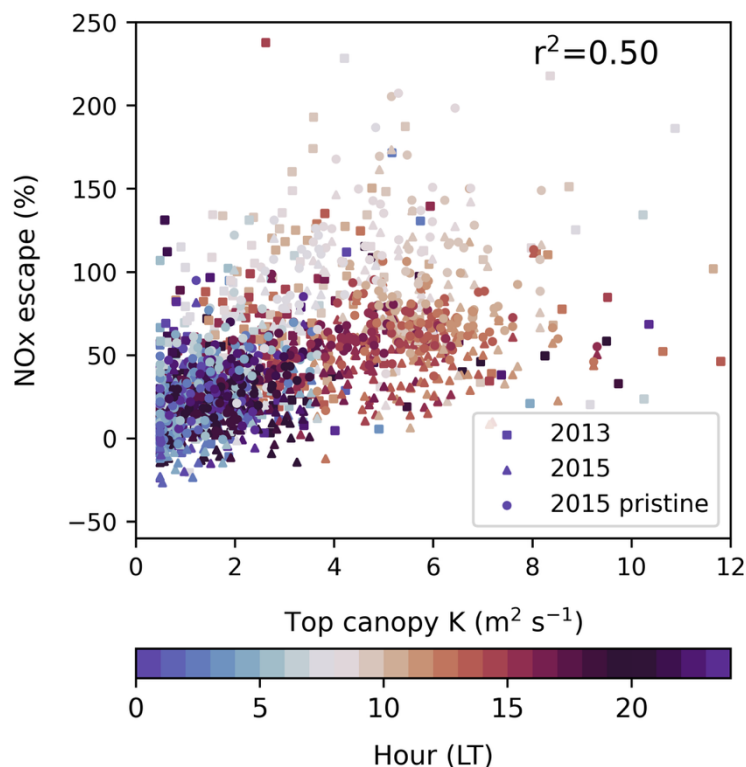


425 Figure 7: Mean diurnal NO_x budget at 35 m of soil NO emissions (grey shading), transfer of upwind transported NO₂ into the
 canopy (red shading), net chemical change (dark green shading), deposition (light green shading) and storage (pink shading)
 within the canopy for (a) the daily mean and (b) – (c) the mean diurnal cycle in individual simulations. (a) 2013, (b) 2015
 including transported NO₂ and (c) 2015 without transported NO₂. In (a), the text gives the escape efficiency. In (b) – (c) The
 sum of all terms except upwind transported NO₂ (black solid line) is the soil NO escape flux.



430 The diurnal cycle of soil NO_x escape at the top of the canopy shows considerable variability over the day, displaying a pronounced cycle that is largely unrelated to diurnal variability in soil NO emissions (Figs. 6b–6d). Daylight hours have the highest escape efficiency, whereas NO_x release overnight is suppressed by in-canopy storage and enhanced deposition. The greatest transfer from the canopy occurs at sunrise when stable separation between the canopy and above breaks down and photochemistry is initiated (Fig. 7, pink shading). This is very pronounced in 2015 when the escape from the canopy is greater than the instantaneous soil emission rate. NO emitted from the soil is rapidly oxidized to NO₂ when O₃ is present, but during 435 the night, NO accumulates near the ground. With the onset of turbulent mixing under daylight, O₃ oxidises NO to NO₂, which is transported upwards but partially taken up by vegetation (Gut et al., 2002; Breuninger et al., 2013; Chaparro-Suarez et al., 2011).

440 Comparing across simulations, we find the escape efficiency in 2013 is lower at all times of day, with a smaller day-night contrast compared to 2015 (Fig. 7b). Over the course of the day, the escape efficiency varies from 25%–100% in 2013 and 30%–130% in 2015. Escape efficiencies over 100% occur when release of stored and emitted NO_x results in canopy fluxes greater than the instantaneous emissions. On the other hand, transport of upwind NO₂ in 2015 does not change the mean diurnal pattern significantly (c.a. Figs. 6c, 6d); the morning storage release is slightly reduced, likely due to a reduced concentration gradient when NO₂ transport occurs.



445

Figure 8: The turbulent exchange parameter K compared to NO_x escape efficiency in simulations of 2013 (square markers), 2015 including transported NO₂ (triangle markers) and 2015 without transported NO₂ (circle markers) in half hourly values. Shading indicated the hour in local time.

450 Figure 8 demonstrates that vertical mixing can largely account for diurnal, daily and between-simulation variability in soil NO_x escape efficiency. There is a correlation between the eddy diffusivity coefficient K and NO_x escape efficiency ($r^2=0.50$) across all simulations at a 30 min time resolution, suggesting half of the variability can be explained by vertical turbulence; longer canopy residence times increase the opportunity for deposition and other chemical losses in addition to in-canopy storage. Most of the variability is diurnal, although differences across days are also explained by the degree of mixing (Fig. 455 S17). Among simulations, the reduced escape efficiency in 2013 relative to 2015 can be related to the slower vertical mixing, whereas the addition of transported NO₂ in 2015 causes an increase in net chemical removal that is unrelated to mixing parameterisations. The morning spike in NO_x escape is not described by K but is the main driver of O₃ production above canopy in pristine conditions (Fig. 6). The concentrated release of NO at sunrise facilitates greater O₃ production than if the same emissions were distributed across the day and is therefore important for capturing O₃ chemistry in pristine conditions.

460 Literature estimates show that NO_x escape efficiencies are poorly constrained by observations. Comparison of single-layer parameterisations by Yienger and Levy (1995) to multilayer canopy calculations by Ganzeveld et al. (2002) find tropical forests are highly sensitive to in-canopy NO_x processes due to the role of chemistry and turbulence within the canopy. While

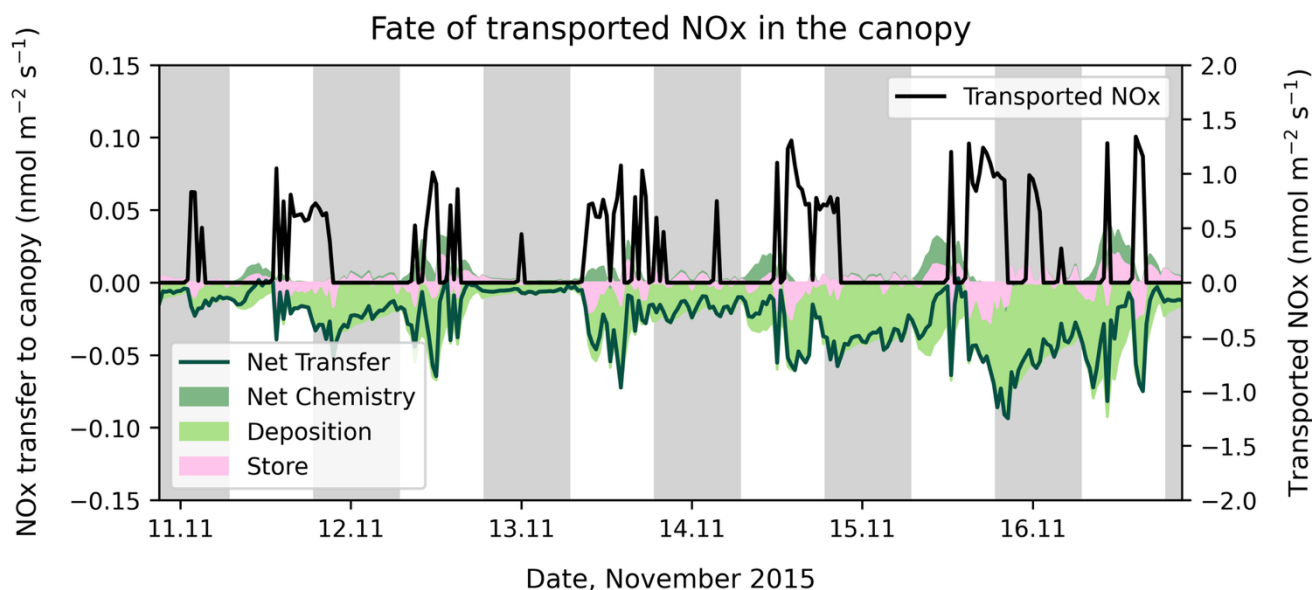


single-layer estimates of 20% likely overestimate the role of deposition, the multilayer average from Ganzeveld et al. (2002) of 40% is closer to our findings. We suggest that turbulence above the canopy is a good indicator of variability at this site
465 without needing to resolve the full canopy structure and that resolution of the diurnal cycle in NO_x escape is most important for representing the majority of the variability in escape efficiency.

3.4.2. The fate of upwind transported NO_x within the canopy

Figure 9 compares the timing of the NO_x transport events above the canopy in 2015 with the eventual transfer to the canopy
470 and fate within the canopy, highlighting the first 6 days of simulation. Most NO_2 transport in the simulation occurs during the day, due to low wind speeds at night.

The instantaneous response to transported NO_x within the canopy is an increase in canopy storage and deposition. After the NO_2 transport ends, there is often a reversal of storage (i.e., a release of NO_x), although enhanced deposition continues. This is especially clear in the daytime of the 16th. During the day, NO_2 transport often results in an almost instant transfer to the
475 canopy, such that the net transfer follows the same pattern as spikes in upwind transport. This is due to efficient mixing into the canopy during the day. During the night, upwind NO_2 transport is not immediately transferred into the canopy, for example overnight transport events on the 13th and 14th do not show up as spikes in net canopy transfer. Instead, deposition is often spread throughout the night, especially if there has been significant transport of NO_2 to the site in the early evening (e.g. night of 15th and 16th). This is in response to NO_2 that was transferred into the canopy during the day and remains trapped due to
480 nighttime stagnation of vertical mixing. In this way, the canopy response to NO_2 transport lasts longer than the actual transport event above the canopy and depends on the time of day. Most resistance-based deposition schemes include an aerodynamic resistance that is lower when vertical turbulence is higher, however this does not account for enhanced deposition of NO_2 during stagnant conditions overnight and may therefore underestimate NO_x losses to the canopy. The transfer into the canopy at individual moments are, at some nighttime hours, greater than the soil NO escape, making the canopy a NO_x sink (Fig.
485 S17b).



490 Figure 9: NO_x transported from upwind above the canopy (black solid line) compared to the transported NO_x entering the canopy (green solid line), divided into deposition (light green shading), net chemistry (dark green shading) and storage (pink shading). Tick marks on the x axis are placed at midnight.

4. Discussion

We demonstrate that a column model at the ATTO site in the remote Amazon successfully captures the greater meteorological and concentration gradients characteristic of deep tropical canopies, expanding previous applications in more well-mixed temperate forest (Ashworth et al., 2015; Wei et al., 2021). Notably, the model successfully simulates a 2-week period whereas
495 previous studies were limited to two days.

The model reveals the critical role of transported precursors from biomass burning in the tropics. The flux of O₃ into the canopy is highest in 2015, attributed to O₃ production above the canopy from transported NO₂ from the Arc of Deforestation. The higher O₃ concentrations lead to greater sesquiterpene ozonolysis, reducing the sesquiterpene escape efficiency (Sect. 3.3.) whilst also decreasing the chemical loss velocity of O₃ (Fig. 4b). This suggests that increased transport of biomass burning
500 pollution reduces the ability of the canopy to remove O₃ from the atmosphere. Because of the higher flux of freshly-formed O₃ into the canopy, absolute deposition and chemical losses increase (Fig. 4a). Biomass burning therefore increases stomatal O₃ flux, leading to a heightened risk of O₃ damage to the forest (e.g., Cheesman et al., 2024). We note that our representation of biomass burning by transport of upwind NO₂ is a substantial simplification; biomass burning is guaranteed to bring other trace gases not included in this simulation, which may impact background composition. Equally, wind arriving from the chosen
505 direction has not necessarily passed through a biomass burning plume. Nonetheless, good representation of day-to-day variability in O₃ concentrations suggests this is a reasonable approximation (Fig. 2b).

Meteorological differences between 2013 and 2015, including higher temperatures and PAR in 2015, enhance BVOC emissions and O₃ deposition velocities but produce only a small increase in chemical and depositional O₃ loss velocities (Fig. 4b). The higher deposition velocities in 2015 suggest no significant stomatal limitation (Fig. 4b). Deposition schemes are highly parameterised and remain a substantial uncertainty in canopy modelling, and this study did not explore the leaf- or soil-level parameterisations in detail. As the majority of simulated O₃ and NO_x canopy losses occur via this pathway, greater focus is needed on accurately representing deposition within the canopy and its response to changing meteorological conditions. Whilst stomata play a crucial role, deposition on plant surfaces also have an influence (Sun et al., 2016), but these are often represented, including here, by simple parameterisations in models.

Vertical turbulent mixing is a major contributor to variability in soil NO_x escape efficiency (Fig. 8) and, to a lesser degree, in the escape efficiency of pool BVOCs and transfer of upwind NO₂ into the canopy; increased residence time within the canopy as a result of reduced mixing increases opportunities for chemical loss and deposition, decreasing escape efficiencies. Qualitatively, vertical mixing profiles are comparable to other measurements at Amazon sites (e.g., Freire et al., 2017; Santana et al., 2018) although representation of downdrafts and large-scale canopy sweeps (Bardakov et al., 2022; Unfer et al., 2025) are not possible with our parameterisation but can dominate the transport process at this site (Cava et al., 2022). For a more explicit representation of vertical mixing processes, large eddy simulations (LES) that include a canopy should be explored (e.g., Pedruzo-Bagazgoitia et al., 2023).

Our simulations repeatedly highlight sesquiterpenes as dominant species in O₃ chemical removal within and above the canopy (Fig. 6). Nonetheless, further measurements of sesquiterpene species and reactivity are needed to accurately quantify the impact on O₃ concentrations. Similarly, monoterpene emissions can include highly reactive species that have not been accurately characterised. We use the reactivity of β -caryophyllene to represent sesquiterpenes in our simulations, a species known for its high reactivity with O₃. This should be considered an upper limit on sesquiterpene contribution to reactivity, and therefore a lower limit on escape efficiency. Although β -caryophyllene is often a dominant species in measurements, farnesene, cadinenes, and muurolenes are frequently found to also be significant (Isaacman-VanWertz et al., 2024). A greater understanding of sesquiterpene emissions composition, and reactivity of other sesquiterpene classes would reduce uncertainty. Measuring the concentration of such highly reactive compounds in the atmosphere is severely hampered by their rapid decomposition; measurements must be taken close to the source. Our simulations also find that O₃ reactivity with sesquiterpenes can continue above 100 m (Fig. 5), which suggests sesquiterpene concentration measurements may be possible above the canopy, especially in pristine conditions, which could help to constrain the model further.

In addition to the BVOCs investigated in this study, recent studies at ATTO show that oxygen-containing VOCs (OVOCs) contribute up to 22%–40% to the average OH reactivity, indicating the complexity of atmospheric oxidation (Ringsdorf et al., 2024), and that OVOCs have been underestimated as an important factor in the OH sink over the Amazon rainforest (Pfanerstill et al., 2021). Measurements at ATTO also show sesquiterpene emission from soils (Bourtsokidis et al., 2018) and cryptogams (Edtbauer et al., 2021): an initial estimate concluded they may contribute up to 10% of carbon emitted as VOCs in the form of highly reactive compounds (Kuhn et al., 2007). The processes from biological production to release to

atmospheric fate, are highly complex, and more work is needed to investigate primary BVOC emissions at the leaf, branch and soil levels, track their atmospheric fate, and explore this complexity using models.

Similarly, the absence of reliable NO_x emissions and concentration measurements at the ATTO site prevents a direct evaluation of NO_x concentrations in the model. Missing σ_w data in 2013 likely also affected the model ability to faithfully simulate individual days. It is possible that by using σ_w from 2015 as a substitute, the average turbulence was too high, since some studies in the Amazon report 2015 as having increased turbulence compared to average years (Carneiro and Fisch, 2020; Pfannerstill et al., 2018). Additional measurements are required to refine the model and evaluate its accuracy under varying conditions across months, years, and seasons. Furthermore, collaborative efforts between observation and modelling studies can help ensure data is collected in a way that is useful for multiple applications.

Finally, we consider the representation of these processes in global chemistry models. Differences in in-canopy O_3 chemistry between 2013 and 2015 in our simulations only cause a small change in total loss velocity, suggesting there is not an urgent need for in-canopy chemical loss parameterisations that vary with environmental conditions. Similarly, explicit quantification of in-canopy sesquiterpene chemistry may not be essential for global modelling of O_3 as simulations without sesquiterpene emissions showed the O_3 + sesquiterpene reactions were compensated for via increased dry deposition (Fig. 4). Most global chemistry models exclude sesquiterpene chemistry due to uncertainties in their reactivity and the assumption that sesquiterpenes are removed within the canopy. Our model suggests that in pristine tropical environments approximately half of emissions can escape from the canopy and therefore may be relevant to boundary layer chemistry in global models, especially in pristine areas such as the tropics. Daily mean sesquiterpene escape efficiencies in our simulations qualitatively agree with existing escape efficiency parameterisations in global canopy-scale models (Guenther et al., 2006). Key factors affecting their escape are the degree of vertical mixing and the O_3 concentration (Fig. S16). For escape efficiencies of monoterpenes and isoprene, species with light-dependent emissions are the least sensitive to changes in in-canopy chemistry due to rapid mixing and equilibration during daylight – changes in oxidative capacity and depositional environment have a greater effect on the mean escape efficiency of species that build up overnight. Existing soil NO_x parameterisations (Yienger and Levy, 1995) estimate greater in-canopy losses than our model; we calculate mean escape efficiencies of 40%–50%. We further highlight that a diurnally varying parameterisation of soil NO_x escape could improve representation of variability in NO_x chemistry; the diurnal cycle of soil NO_x escape is strongly related to vertical turbulence, combined with an additional spike in morning escape efficiency that is important to consider for accurate simulation of O_3 production (Fig. 7).

5. Conclusion

Our column model application at the ATTO site successfully resolves key processes governing canopy–atmosphere exchange in the Amazon rainforest. The simulations capture interannual variability between 2013 and the 2015/16 El Niño and reveal a previously underappreciated role of biomass burning in modulating canopy chemistry. Precursor transport from biomass burning enhances O_3 concentrations, reduces BVOC and NO_x escape efficiencies, and alters O_3 chemical loss pathways. Sesquiterpenes, though exerting limited influence on total O_3 fluxes, play a key role in partitioning between chemical and



depositional removal, introducing uncertainty due to poorly constrained emissions and reactivity. The uncertainty surrounding
575 the role of sesquiterpenes is extremely high and research suggests that there are likely more sources than we include here.
Variability in vertical mixing emerges as a dominant driver of both BVOC and NO_x escape efficiencies, with implications for
how these processes are represented in larger-scale models. Despite reasonable agreement with observations, uncertainties
remain in emission magnitudes, chemical reactivity, and deposition parameterisations, emphasising the need for expanded in
situ measurements, particularly of sesquiterpenes and soil NO_x fluxes. Future work coupling column or LES frameworks that
580 include vegetation with long-term, multi-seasonal datasets will be essential to refine canopy exchange parameterisations and
to improve predictions of tropical forest responses to climatic and atmospheric perturbations. Given the potential for shifts in
fire activity, dry season length, and BVOC emissions under future climate scenarios, improved treatment of in-canopy
processes will be essential for constraining tropical atmospheric chemistry and its role in regional and global oxidant budgets.

585 **Data availability:** Data and scripts to reproduce all figures will be stored with DOI on a Zenodo archive following review.
The column model with adaptations for the ATTO site is available on github (https://github.com/flossie-brown/FORCAsT_ATTO).
Observation data is available at www.attodata.org.

Author contribution:

590 Conceptualisation: FB, CLH
Supervision: CLH
Analysis & Visualisation: FB
Writing – first draft: FB
Writing: FB, CLH
595 Resources: AS, HH, CAM, AMYS, JK, ACA, CQDJ, DHH
Writing – review & editing: all authors

Competing interests: The authors declare that they have no conflict of interest.

Acknowledgements: ATTO scientists thank the Instituto Nacional de Pesquisas da Amazonia (INPA) and the Max Planck
600 Society for continuous support. We acknowledge the support by the German Federal Ministry of Education and Research
(BMBF contracts 01LB1001A and 01LK1602B) and the Brazilian Ministério da Ciência, Tecnologia e Inovação
(MCTI/FINEP contract 01.11.01248.00) as well as the Amazon State University (UEA), FAPEAM, LBA/INPA and
SDS/CEUC/RDS-Uatumã.)

References

605 Andreae, M. O., Acevedo, O. C., Araújo, A., Artaxo, P., Barbosa, C. G. G., Barbosa, H. M. J., Brito, J., Carbone, S., Chi, X.,
Cintra, B. B. L., da Silva, N. F., Dias, N. L., Dias-Júnior, C. Q., Ditas, F., Ditz, R., Godoi, A. F. L., Godoi, R. H. M., Heimann,



- M., Hoffmann, T., Kesselmeier, J., Könemann, T., Krüger, M. L., Lavric, J. V., Manzi, A. O., Lopes, A. P., Martins, D. L., Mikhailov, E. F., Moran-Zuloaga, D., Nelson, B. W., Nölscher, A. C., Santos Nogueira, D., Piedade, M. T. F., Pöhlker, C., Pöschl, U., Quesada, C. A., Rizzo, L. V., Ro, C.-U., Ruckteschler, N., Sá, L. D. A., de Oliveira Sá, M., Sales, C. B., dos Santos, R. M. N., Saturno, J., Schöngart, J., Sörgel, M., de Souza, C. M., de Souza, R. a. F., Su, H., Targhetta, N., Tóta, J., Trebs, I., Trumbore, S., van Eijck, A., Walter, D., Wang, Z., Weber, B., Williams, J., Winderlich, J., Wittmann, F., Wolff, S., and Yáñez-Serrano, A. M.: The Amazon Tall Tower Observatory (ATTO): overview of pilot measurements on ecosystem ecology, meteorology, trace gases, and aerosols, *Atmospheric Chemistry and Physics*, 15, 10723–10776, <https://doi.org/10.5194/acp-15-10723-2015>, 2015.
- 615 Aragão, L. E., Anderson, L. O., Fonseca, M. G., Rosan, T. M., Vedovato, L. B., Wagner, F. H., Silva, C. V., Silva Junior, C. H., Arai, E., and Aguiar, A. P.: 21st Century drought-related fires counteract the decline of Amazon deforestation carbon emissions, *Nature communications*, 9, 536, 2018.
- Ashworth, K., Chung, S. H., Griffin, R. J., Chen, J., Forkel, R., Bryan, A. M., and Steiner, A. L.: FORest Canopy Atmosphere Transfer (FORCAST) 1.0: a 1-D model of biosphere–atmosphere chemical exchange, *Geosci. Model Dev.*, 8, 3765–3784, <https://doi.org/10.5194/gmd-8-3765-2015>, 2015.
- 620 Bardakov, R., Krejci, R., Riipinen, I., and Ekman, A. M. L.: The Role of Convective Up- and Downdrafts in the Transport of Trace Gases in the Amazon, *Journal of Geophysical Research: Atmospheres*, 127, e2022JD037265, <https://doi.org/10.1029/2022JD037265>, 2022.
- Bourtsoukidis, E., Behrendt, T., Yáñez-Serrano, A. M., Hellén, H., Diamantopoulos, E., Catão, E., Ashworth, K., Pozzer, A., Quesada, C. A., Martins, D. L., Sá, M., Araujo, A., Brito, J., Artaxo, P., Kesselmeier, J., Lelieveld, J., and Williams, J.: Strong sesquiterpene emissions from Amazonian soils, *Nat Commun*, 9, 2226, <https://doi.org/10.1038/s41467-018-04658-y>, 2018.
- 625 Breuninger, C., Meixner, F. X., and Kesselmeier, J.: Field investigations of nitrogen dioxide (NO₂) exchange between plants and the atmosphere, *Atmospheric Chemistry and Physics*, 13, 773–790, <https://doi.org/10.5194/acp-13-773-2013>, 2013.
- Brown, F., Folberth, G. A., Sitch, S., Bauer, S., Bauters, M., Boeckx, P., Cheesman, A. W., Deushi, M., Dos Santos Vieira, I., Galy-Lacaux, C., Haywood, J., Keeble, J., Mercado, L. M., O’Connor, F. M., Oshima, N., Tsigaridis, K., and Verbeek, H.: The ozone–climate penalty over South America and Africa by 2100, *Atmospheric Chemistry and Physics*, 22, 12331–12352, <https://doi.org/10.5194/acp-22-12331-2022>, 2022.
- 630 Bryan, A. M., Bertman, S. B., Carroll, M. A., Dusanter, S., Edwards, G. D., Forkel, R., Griffith, S., Guenther, A. B., Hansen, R. F., Helmig, D., Jobson, B. T., Keutsch, F. N., Lefér, B. L., Pressley, S. N., Shepson, P. B., Stevens, P. S., and Steiner, A. L.: In-canopy gas-phase chemistry during CABINEX 2009: sensitivity of a 1-D canopy model to vertical mixing and isoprene chemistry, *Atmospheric Chemistry and Physics*, 12, 8829–8849, <https://doi.org/10.5194/acp-12-8829-2012>, 2012.
- Carneiro, R. G. and Fisch, G.: Observational analysis of the daily cycle of the planetary boundary layer in the central Amazon during a non-El Niño year and El Niño year (GoAmazon project 2014/5), *Atmospheric Chemistry and Physics*, 20, 5547–5558, <https://doi.org/10.5194/acp-20-5547-2020>, 2020.
- 640 Cava, D., Dias-Júnior, C. Q., Acevedo, O., Oliveira, P. E. S., Tsokankunku, A., Sörgel, M., Manzi, A. O., de Araújo, A. C., Brondani, D. V., Toro, I. M. C., and Mortarini, L.: Vertical propagation of submeso and coherent structure in a tall and dense Amazon Forest in different stability conditions PART I: Flow structure within and above the roughness sublayer, *Agricultural and Forest Meteorology*, 322, 108983, <https://doi.org/10.1016/j.agrformet.2022.108983>, 2022.
- 645 Chamecki, M., Freire, L. S., Dias, N. L., Chen, B., Dias-Junior, C. Q., Machado, L. A. T., Sörgel, M., Tsokankunku, A., and Araújo, A. C. de: Effects of Vegetation and Topography on the Boundary Layer Structure above the Amazon Forest, *Journal of the Atmospheric Sciences*, 77, 2941–2957, <https://doi.org/10.1175/JAS-D-20-0063.1>, 2020.



- Chaparro-Suarez, I. G., Meixner, F. X., and Kesselmeier, J.: Nitrogen dioxide (NO₂) uptake by vegetation controlled by atmospheric concentrations and plant stomatal aperture, *Atmospheric Environment*, 45, 5742–5750, <https://doi.org/10.1016/j.atmosenv.2011.07.021>, 2011.
- 650 Cheesman, A. W., Brown, F., Artaxo, P., Farha, M. N., Folberth, G. A., Hayes, F. J., Heinrich, V. H., Hill, T. C., Mercado, L. M., and Oliver, R. J.: Reduced productivity and carbon drawdown of tropical forests from ground-level ozone exposure, *Nature Geoscience*, 17, 1003–1007, 2024.
- Costa, B., Anselmo-Moreira, F., Nascimento, A., Pedrosa, G., Catharino, E., Borbon, A., Fornaro, A., Furlan, C., and Souza, S. de: Unveiling Sesquiterpene Emissions in Dominant Trees of a Brazilian Atlantic Forest Remnant, <https://doi.org/10.26434/chemrxiv-2025-8pg46>, 17 April 2025.
- 655 Covey, K., Soper, F., Pangala, S., Bernardino, A., Pagliaro, Z., Basso, L., Cassol, H., Fearnside, P., Navarrete, D., Novoa, S., Sawakuchi, H., Lovejoy, T., Marengo, J., Peres, C. A., Baillie, J., Bernasconi, P., Camargo, J., Freitas, C., Hoffman, B., Nardoto, G. B., Nobre, I., Mayorga, J., Mesquita, R., Pavan, S., Pinto, F., Rocha, F., de Assis Mello, R., Thuault, A., Bahl, A. A., and Elmore, A.: Carbon and Beyond: The Biogeochemistry of Climate in a Rapidly Changing Amazon, *Front. For. Glob. Change*, 4, <https://doi.org/10.3389/ffgc.2021.618401>, 2021.
- 660 Dias-Júnior, C. Q., Dias, N. L., dos Santos, R. M. N., Sörgel, M., Araújo, A., Tsokankunku, A., Ditas, F., de Santana, R. A., von Randow, C., Sá, M., Pöhlker, C., Toledo Machado, L. A., de Sá, L. D., Moran-Zuloaga, D., Janssen, R., Acevedo, O., Oliveira, P., Fisch, G., Chor, T., and Manzi, A.: Is There a Classical Inertial Sublayer Over the Amazon Forest?, *Geophysical Research Letters*, 46, 5614–5622, <https://doi.org/10.1029/2019GL083237>, 2019.
- 665 Edtbauer, A., Pfannerstill, E. Y., Pires Florentino, A. P., Barbosa, C. G. G., Rodriguez-Caballero, E., Zannoni, N., Alves, R. P., Wolff, S., Tsokankunku, A., Aptroot, A., de Oliveira Sá, M., de Araújo, A. C., Sörgel, M., de Oliveira, S. M., Weber, B., and Williams, J.: Cryptogamic organisms are a substantial source and sink for volatile organic compounds in the Amazon region, *Commun Earth Environ*, 2, 258, <https://doi.org/10.1038/s43247-021-00328-y>, 2021.
- 670 Forkel, R., Klemm, O., Graus, M., Rappenglück, B., Stockwell, W. R., Grabmer, W., Held, A., Hansel, A., and Steinbrecher, R.: Trace gas exchange and gas phase chemistry in a Norway spruce forest: A study with a coupled 1-dimensional canopy atmospheric chemistry emission model, *Atmospheric Environment*, 40, 28–42, <https://doi.org/10.1016/j.atmosenv.2005.11.070>, 2006.
- Freire, L. S., Gerken, T., Ruiz-Plancarte, J., Wei, D., Fuentes, J. D., Katul, G. G., Dias, N. L., Acevedo, O. C., and Chamecki, M.: Turbulent mixing and removal of ozone within an Amazon rainforest canopy, *Journal of Geophysical Research: Atmospheres*, 122, 2791–2811, <https://doi.org/10.1002/2016JD026009>, 2017.
- 675 Ganzeveld, L. N., Lelieveld, J., Dentener, F. J., Krol, M. C., Bouwman, A. J., and Roelofs, G.-J.: Global soil-biogenic NO_x emissions and the role of canopy processes, *Journal of Geophysical Research: Atmospheres*, 107, ACH 9-1-ACH 9-17, <https://doi.org/10.1029/2001JD001289>, 2002.
- 680 Gao, W., Wesely, M. L., and Doskey, P. V.: Numerical modeling of the turbulent diffusion and chemistry of NO_x, O₃, isoprene, and other reactive trace gases in and above a forest canopy, *Journal of Geophysical Research: Atmospheres*, 98, 18339–18353, <https://doi.org/10.1029/93JD01862>, 1993.
- Gomes Alves, E., Taylor, T., Robin, M., Pinheiro Oliveira, D., Schiatti, J., Duvoisin Júnior, S., Zannoni, N., Williams, J., Hartmann, C., Gonçalves, J. F. C., Schöngart, J., Wittmann, F., and Piedade, M. T. F.: Seasonal shifts in isoprenoid emission composition from three hyperdominant tree species in central Amazonia, *Plant Biology*, 24, 721–733, <https://doi.org/10.1111/plb.13419>, 2022.



- 685 Gomes Alves, E., Aquino Santana, R., Quaresma Dias-Júnior, C., Botía, S., Taylor, T., Yáñez-Serrano, A. M., Kesselmeier, J., Bourtsoukidis, E., Williams, J., Lembo Silveira de Assis, P. I., Martins, G., de Souza, R., Duvoisin Júnior, S., Guenther, A., Gu, D., Tsokankunku, A., Sörgel, M., Nelson, B., Pinto, D., Komiya, S., Martins Rosa, D., Weber, B., Barbosa, C., Robin, M., Feeley, K. J., Duque, A., Londoño Lemos, V., Contreras, M. P., Idarraga, A., López, N., Husby, C., Jestrow, B., and Cely Toro, I. M.: Intra- and interannual changes in isoprene emission from central Amazonia, *Atmospheric Chemistry and Physics*, 23, 8149–8168, <https://doi.org/10.5194/acp-23-8149-2023>, 2023.
- 690 Guenther, A., Hewitt, C. N., Erickson, D., Fall, R., Geron, C., Graedel, T., Harley, P., Klinger, L., Lerdau, M., Mckay, W. A., Pierce, T., Scholes, B., Steinbrecher, R., Tallamraju, R., Taylor, J., and Zimmerman, P.: A global model of natural volatile organic compound emissions, *Journal of Geophysical Research: Atmospheres*, 100, 8873–8892, <https://doi.org/10.1029/94JD02950>, 1995.
- 695 Guenther, A., Karl, T., Harley, P., Wiedinmyer, C., Palmer, P. I., and Geron, C.: Estimates of global terrestrial isoprene emissions using MEGAN (Model of Emissions of Gases and Aerosols from Nature), *Atmospheric Chemistry and Physics*, 6, 3181–3210, <https://doi.org/10.5194/acp-6-3181-2006>, 2006.
- Guenther, A. B., Jiang, X., Heald, C. L., Sakulyanontvittaya, T., Duhl, T., Emmons, L. K., and Wang, X.: The Model of Emissions of Gases and Aerosols from Nature version 2.1 (MEGAN2.1): an extended and updated framework for modeling biogenic emissions, *Geoscientific Model Development*, 5, 1471–1492, <https://doi.org/10.5194/gmd-5-1471-2012>, 2012.
- 700 Gut, A., Scheibe, M., Rottenberger, S., Rummel, U., Welling, M., Ammann, C., Kirkman, G. A., Kuhn, U., Meixner, F. X., Kesselmeier, J., Lehmann, B. E., Schmidt, W., Müller, E., and Piedade, M. T. F.: Exchange fluxes of NO₂ and O₃ at soil and leaf surfaces in an Amazonian rain forest, *Journal of Geophysical Research: Atmospheres*, 107, LBA 27-1-LBA 27-15, <https://doi.org/10.1029/2001JD000654>, 2002.
- 705 Isaacman-VanWertz, G., Frazier, G., Willison, J., and Faiola, C.: Missing Measurements of Sesquiterpene Ozonolysis Rates and Composition Limit Understanding of Atmospheric Reactivity, *Environ. Sci. Technol.*, <https://doi.org/10.1021/acs.est.3c10348>, 2024.
- Jardine, K., Yáñez Serrano, A., Arneth, A., Abrell, L., Jardine, A., van Haren, J., Artaxo, P., Rizzo, L. V., Ishida, F. Y., Karl, T., Kesselmeier, J., Saleska, S., and Huxman, T.: Within-canopy sesquiterpene ozonolysis in Amazonia, *Journal of Geophysical Research: Atmospheres*, 116, <https://doi.org/10.1029/2011JD016243>, 2011.
- 710 Jarvis, A. J., Mansfield, T. A., and Davies, W. J.: Stomatal behaviour, photosynthesis and transpiration under rising CO₂, *Plant, Cell & Environment*, 22, 639–648, <https://doi.org/10.1046/j.1365-3040.1999.00407.x>, 1999.
- Jiménez-Muñoz, J. C., Mattar, C., Barichivich, J., Santamaría-Artigas, A., Takahashi, K., Malhi, Y., Sobrino, J. A., and Schrier, G. van der: Record-breaking warming and extreme drought in the Amazon rainforest during the course of El Niño 2015–2016, *Sci Rep*, 6, 33130, <https://doi.org/10.1038/srep33130>, 2016.
- 715 Kuhn, U., Rottenberger, S., Biesenthal, T., Wolf, A., Schebeske, G., Ciccioli, P., Brancaleoni, E., Frattoni, M., Tavares, T. M., and Kesselmeier, J.: Seasonal differences in isoprene and light-dependent monoterpene emission by Amazonian tree species, *Global Change Biology*, 10, 663–682, <https://doi.org/10.1111/j.1529-8817.2003.00771.x>, 2004a.
- 720 Kuhn, U., Rottenberger, S., Biesenthal, T., Wolf, A., Schebeske, G., Ciccioli, P., and Kesselmeier, J.: Strong correlation between isoprene emission and gross photosynthetic capacity during leaf phenology of the tropical tree species *Hymenaea courbaril* with fundamental changes in volatile organic compounds emission composition during early leaf development, *Plant, Cell & Environment*, 27, 1469–1485, <https://doi.org/10.1111/j.1365-3040.2004.01252.x>, 2004b.



- 725 Kuhn, U., Andreae, M. O., Ammann, C., Araújo, A. C., Brancaleoni, E., Ciccioli, P., Dindorf, T., Frattoni, M., Gatti, L. V., Ganzeveld, L., Kruijt, B., Lelieveld, J., Lloyd, J., Meixner, F. X., Nobre, A. D., Pöschl, U., Spirig, C., Stefani, P., Thielmann, A., Valentini, R., and Kesselmeier, J.: Isoprene and monoterpene fluxes from Central Amazonian rainforest inferred from tower-based and airborne measurements, and implications on the atmospheric chemistry and the local carbon budget, *Atmospheric Chemistry and Physics*, 7, 2855–2879, <https://doi.org/10.5194/acp-7-2855-2007>, 2007.
- 730 Makar, P. A., Staebler, R. M., Akingunola, A., Zhang, J., McLinden, C., Kharol, S. K., Pabla, B., Cheung, P., and Zheng, Q.: The effects of forest canopy shading and turbulence on boundary layer ozone, *Nat Commun*, 8, 15243, <https://doi.org/10.1038/ncomms15243>, 2017.
- Marengo, J. A., Souza, C. M., Thonicke, K., Burton, C., Halladay, K., Betts, R. A., Alves, L. M., and Soares, W. R.: Changes in Climate and Land Use Over the Amazon Region: Current and Future Variability and Trends, *Front. Earth Sci.*, 6, <https://doi.org/10.3389/feart.2018.00228>, 2018.
- 735 Meyers, T. P. and Baldocchi, D. D.: A comparison of models for deriving dry deposition fluxes of O₃ and SO₂ to a forest canopy, *Tellus B*, 40B, 270–284, <https://doi.org/10.1111/j.1600-0889.1988.tb00297.x>, 1988.
- Norman, J.: Modeling the complete crop canopy., 1979.
- Pacifico, F., Folberth, G., Sitch, S., Haywood, J., Rizzo, L., Malavelle, F., and Artaxo, P.: Biomass burning related ozone damage on vegetation over the Amazon forest: a model sensitivity study, *Atmospheric Chemistry and Physics*, 15, 2791–2804, 2015.
- 740 Pedruzo-Bagazgoitia, X., Patton, E. G., Moene, A. F., Ouwersloot, H. G., Gerken, T., Machado, L. a. T., Martin, S. T., Sörgel, M., Stoy, P. C., Yamasoe, M. A., and Vilà-Guerau de Arellano, J.: Investigating the Diurnal Radiative, Turbulent, and Biophysical Processes in the Amazonian Canopy-Atmosphere Interface by Combining LES Simulations and Observations, *Journal of Advances in Modeling Earth Systems*, 15, e2022MS003210, <https://doi.org/10.1029/2022MS003210>, 2023.
- 745 Pfannerstill, E. Y., Nölscher, A. C., Yáñez-Serrano, A. M., Bourtsoukidis, E., Keßel, S., Janssen, R. H. H., Tsokankunku, A., Wolff, S., Sörgel, M., Sá, M. O., Araújo, A., Walter, D., Lavrič, J., Dias-Júnior, C. Q., Kesselmeier, J., and Williams, J.: Total OH Reactivity Changes Over the Amazon Rainforest During an El Niño Event, *Front. For. Glob. Change*, 1, <https://doi.org/10.3389/ffgc.2018.00012>, 2018.
- 750 Pfannerstill, E. Y., Reijrink, N. G., Edtbauer, A., Ringsdorf, A., Zannoni, N., Araújo, A., Ditas, F., Holanda, B. A., Sá, M. O., Tsokankunku, A., Walter, D., Wolff, S., Lavrič, J. V., Pöhlker, C., Sörgel, M., and Williams, J.: Total OH reactivity over the Amazon rainforest: variability with temperature, wind, rain, altitude, time of day, season, and an overall budget closure, *Atmospheric Chemistry and Physics*, 21, 6231–6256, <https://doi.org/10.5194/acp-21-6231-2021>, 2021.
- 755 Pöhlker, C., Walter, D., Paulsen, H., Könemann, T., Rodríguez-Caballero, E., Moran-Zuloaga, D., Brito, J., Carbone, S., Degrendele, C., Després, V. R., Ditas, F., Holanda, B. A., Kaiser, J. W., Lammel, G., Lavrič, J. V., Ming, J., Pickersgill, D., Pöhlker, M. L., Praß, M., Löbs, N., Saturno, J., Sörgel, M., Wang, Q., Weber, B., Wolff, S., Artaxo, P., Pöschl, U., and Andreae, M. O.: Land cover and its transformation in the backward trajectory footprint region of the Amazon Tall Tower Observatory, *Atmospheric Chemistry and Physics*, 19, 8425–8470, <https://doi.org/10.5194/acp-19-8425-2019>, 2019.
- 760 Pope, R. J., Arnold, S. R., Chipperfield, M. P., Reddington, C. L. S., Butt, E. W., Keslake, T. D., Feng, W., Latter, B. G., Kerridge, B. J., Siddans, R., Rizzo, L., Artaxo, P., Sadiq, M., and Tai, A. P. K.: Substantial Increases in Eastern Amazon and Cerrado Biomass Burning-Sourced Tropospheric Ozone, *Geophysical Research Letters*, 47, e2019GL084143, <https://doi.org/10.1029/2019GL084143>, 2020.



Pugliese, G., Ingrisch, J., Meredith, L. K., Pfannerstill, E. Y., Klüpfel, T., Meeran, K., Byron, J., Purser, G., Gil-Loaiza, J., van Haren, J., Dontsova, K., Kreuzwieser, J., Ladd, S. N., Werner, C., and Williams, J.: Effects of drought and recovery on soil volatile organic compound fluxes in an experimental rainforest, *Nat Commun*, 14, 5064, <https://doi.org/10.1038/s41467-023-40661-8>, 2023.

765 Raupach, M. R.: A practical Lagrangian method for relating scalar concentrations to source distributions in vegetation canopies, *Quarterly Journal of the Royal Meteorological Society*, 115, 609–632, <https://doi.org/10.1002/qj.49711548710>, 1989.

dos Reis, M., Graça, P. M. L. de A., Yanai, A. M., Ramos, C. J. P., and Fearnside, P. M.: Forest fires and deforestation in the central Amazon: Effects of landscape and climate on spatial and temporal dynamics, *Journal of Environmental Management*, 288, 112310, <https://doi.org/10.1016/j.jenvman.2021.112310>, 2021.

770 Ribeiro Neto, G. G., Anderson, L. O., Barretos, N. J. C., Abreu, R., Alves, L., Dong, B., Lott, F. C., and Tett, S. F. B.: Attributing the 2015/2016 Amazon basin drought to anthropogenic influence, *Climate Resilience and Sustainability*, 1, e25, <https://doi.org/10.1002/cli2.25>, 2022.

Ringsdorf, A., Edtbauer, A., Holanda, B., Poehlker, C., Sá, M. O., Araújo, A., Kesselmeier, J., Lelieveld, J., and Williams, J.: Investigating carbonyl compounds above the Amazon rainforest using a proton-transfer-reaction time-of-flight mass spectrometer (PTR-ToF-MS) with NO⁺ chemical ionization, *Atmospheric Chemistry and Physics*, 24, 11883–11910, <https://doi.org/10.5194/acp-24-11883-2024>, 2024.

Rummel, U., Ammann, C., Kirkman, G. A., Moura, M. a. L., Foken, T., Andreae, M. O., and Meixner, F. X.: Seasonal variation of ozone deposition to a tropical rain forest in southwest Amazonia, *Atmospheric Chemistry and Physics*, 7, 5415–5435, <https://doi.org/10.5194/acp-7-5415-2007>, 2007.

780 Santana, R. A., Dias-Júnior, C. Q., da Silva, J. T., Fuentes, J. D., do Vale, R. S., Alves, E. G., dos Santos, R. M. N., and Manzi, A. O.: Air turbulence characteristics at multiple sites in and above the Amazon rainforest canopy, *Agricultural and Forest Meteorology*, 260–261, 41–54, <https://doi.org/10.1016/j.agrformet.2018.05.027>, 2018.

Schmitt, A. U., Ament, F., de Araújo, A. C., Sá, M., and Teixeira, P.: Modeling atmosphere–land interactions at a rainforest site – a case study using Amazon Tall Tower Observatory (ATTO) measurements and reanalysis data, *Atmospheric Chemistry and Physics*, 23, 9323–9346, <https://doi.org/10.5194/acp-23-9323-2023>, 2023.

Serra-Neto, E. M., Martins, H. S., Dias-Júnior, C. Q., Santana, R. A., Brondani, D. V., Manzi, A. O., de Araújo, A. C., Teixeira, P. R., Sörgel, M., and Mortarini, L.: Simulation of the Scalar Transport above and within the Amazon Forest Canopy, *Atmosphere*, 12, 1631, <https://doi.org/10.3390/atmos12121631>, 2021.

790 Silva Junior, C. H. L., Anderson, L. O., Silva, A. L., Almeida, C. T., Dalagnol, R., Pletsch, M. A. J. S., Penha, T. V., Paloschi, R. A., and Aragão, L. E. O. C.: Fire Responses to the 2010 and 2015/2016 Amazonian Droughts, *Front. Earth Sci.*, 7, <https://doi.org/10.3389/feart.2019.00097>, 2019.

Stroud, C., Makar, P., Karl, T., Guenther, A., Geron, C., Turnipseed, A., Nemitz, E., Baker, B., Potosnak, M., and Fuentes, J. D.: Role of canopy-scale photochemistry in modifying biogenic-atmosphere exchange of reactive terpene species: Results from the CELTIC field study, *Journal of Geophysical Research: Atmospheres*, 110, <https://doi.org/10.1029/2005JD005775>, 2005.

795 Sun, S., Moravek, A., Trebs, I., Kesselmeier, J., and Sörgel, M.: Investigation of the influence of liquid surface films on O₃ and PAN deposition to plant leaves coated with organic/inorganic solution, *Journal of Geophysical Research: Atmospheres*, 121, 14,239–14,256, <https://doi.org/10.1002/2016JD025519>, 2016.



- 800 Unfer, G. R., Machado, L. A. T., Albrecht, R. I., Cecchini, M. A., Harder, H., Magina, F. C., Pöhlker, M. L., Pöschl, U., Vilà-Guerau de Arellano, J., Williams, E. R., Wolff, S., and Pöhlker, C.: Decoding the Relationship Between Cloud Electrification, Downdrafts, and Surface Ozone in the Amazon Basin, *Journal of Geophysical Research: Atmospheres*, 130, e2024JD042158, <https://doi.org/10.1029/2024JD042158>, 2025.
- 805 Vieira, I., Verbeeck, H., Meunier, F., Peaucelle, M., Sibret, T., Lefevre, L., Cheesman, A. W., Brown, F., Sitch, S., Mbifo, J., Boeckx, P., and Bauters, M.: Global reanalysis products cannot reproduce seasonal and diurnal cycles of tropospheric ozone in the Congo Basin, *Atmospheric Environment*, 304, 119773, <https://doi.org/10.1016/j.atmosenv.2023.119773>, 2023.
- Visser, A. J., Ganzeveld, L. N., Goded, I., Krol, M. C., Mammarella, I., Manca, G., and Boersma, K. F.: Ozone deposition impact assessments for forest canopies require accurate ozone flux partitioning on diurnal timescales, *Atmospheric Chemistry and Physics*, 21, 18393–18411, <https://doi.org/10.5194/acp-21-18393-2021>, 2021.
- 810 Visser, A. J., Ganzeveld, L. N., Finco, A., Krol, M. C., Marzuoli, R., and Boersma, K. F.: The Combined Impact of Canopy Stability and Soil NO_x Exchange on Ozone Removal in a Temperate Deciduous Forest, *Journal of Geophysical Research: Biogeosciences*, 127, e2022JG006997, <https://doi.org/10.1029/2022JG006997>, 2022.
- 815 Wei, D., Alwe, H. D., Millet, D. B., Bottorff, B., Lew, M., Stevens, P. S., Shutter, J. D., Cox, J. L., Keutsch, F. N., Shi, Q., Kavassalis, S. C., Murphy, J. G., Vasquez, K. T., Allen, H. M., Praske, E., Crouse, J. D., Wennberg, P. O., Shepson, P. B., Bui, A. A. T., Wallace, H. W., Griffin, R. J., May, N. W., Connor, M., Slade, J. H., Pratt, K. A., Wood, E. C., Rollings, M., Deming, B. L., Anderson, D. C., and Steiner, A. L.: FORest Canopy Atmosphere Transfer (FORCAsT) 2.0: model updates and evaluation with observations at a mixed forest site, *Geoscientific Model Development*, 14, 6309–6329, <https://doi.org/10.5194/gmd-14-6309-2021>, 2021.
- 820 Wennberg, P. O., Bates, K. H., Crouse, J. D., Dodson, L. G., McVay, R. C., Mertens, L. A., Nguyen, T. B., Praske, E., Schwantes, R. H., Smarte, M. D., St Clair, J. M., Teng, A. P., Zhang, X., and Seinfeld, J. H.: Gas-Phase Reactions of Isoprene and Its Major Oxidation Products, *Chem. Rev.*, 118, 3337–3390, <https://doi.org/10.1021/acs.chemrev.7b00439>, 2018.
- Wesely, M. L. and Hicks, B. B.: A review of the current status of knowledge on dry deposition, *Atmospheric Environment*, 34, 2261–2282, [https://doi.org/10.1016/S1352-2310\(99\)00467-7](https://doi.org/10.1016/S1352-2310(99)00467-7), 2000.
- 825 Yáñez-Serrano, A. M., Nölscher, A. C., Williams, J., Wolff, S., Alves, E., Martins, G. A., Bourtsoukidis, E., Brito, J., Jardine, K., Artaxo, P., and Kesselmeier, J.: Diel and seasonal changes of biogenic volatile organic compounds within and above an Amazonian rainforest, *Atmospheric Chemistry and Physics*, 15, 3359–3378, <https://doi.org/10.5194/acp-15-3359-2015>, 2015.
- 830 Yáñez-Serrano, A. M., Nölscher, A. C., Bourtsoukidis, E., Gomes Alves, E., Ganzeveld, L., Bonn, B., Wolff, S., Sa, M., Yamasoe, M., Williams, J., Andreae, M. O., and Kesselmeier, J.: Monoterpene chemical speciation in a tropical rainforest: variation with season, height, and time of day at the Amazon Tall Tower Observatory (ATTO), *Atmospheric Chemistry and Physics*, 18, 3403–3418, <https://doi.org/10.5194/acp-18-3403-2018>, 2018.
- Yienger, J. and Levy, H.: Empirical model of global soil-biogenic NO_x emissions, *Journal of Geophysical Research: Atmospheres*, 100, 11447–11464, 1995.